بسم الله الرحمن الرحيم

Sudan University of Science and Technology

Collage of Graduate studies

Diagnostic Performance of MRI, MRS and Perfusion weighted in Characterization of Brain Tumors

الاداء التشخيصي للرنين والمطياف المغنطيسي والوزن الإروائي لتوصيف أورام المخ

A thesis submitted For The Requirements of the Fulfillment to Award Ph.D. Degree in the Diagnostic Radiological Technology

By:

Sabri Abdurrahman Ibrahim Hamed

Supervised by:

Prof.: Caroline Edward Ayad Khilla

July 2019

بسم الله الرحمن الرحيم

قال الله تعالى (يُؤْتِي الْحِكْمَةَ مَنْ يَشَاءُ وَمَنْ يُؤْتَ الْحِكْمَةَ فَقَدْ أُوتِيَ خَيْراً كَثِيراً وَمَا يَذَّكَّرُ إِلاَّ أُوْلُوا الأَلْبَابِ)

البقرة: ٢٦٩

صدق الله العظيم

DEDICATION

To my parents, my wife, and sons for their unwavering encouragement and support along my long journey through my research.

ACKNOWLEDGMENT

I am grateful to God who gave me determination, strength, and potency to evaluate and assess the information of my study and investigation. I am extremely thankful to my supervisor [Prof. Caroline Edward] who developed my abilities with her advices and motivation. The knowledge and skills of my supervisor have always been a source of motivation for me. Her advices resulted in the deletions and additions in the original work.

I would like to express my sincerely thank the participants without whom the study would not have been feasible. The Sudan University of Science and Technology, College of Medical Radiological Science and Neuro-Surgery and Oncology Department at Jazan- Saudi Arabia are thankfully acknowledged.

Abstract

The objectives of this study were to evaluate the effectiveness of perfusion and magnetic resonance spectroscopy in the characterization of brain tumors. And to evaluate the usefulness of MR spectroscopy (MRS) in grading of brain tumors as well to evaluate which metabolite values/ratios could provide better classification/grading of brain tumors when using, short or long TE. The study was conducted during the period extended from 2014 up to 2017, using 1.5 Tesla superconducting Syngo MRI system at Neuro-Surgery and Oncology department at Jazan- Saudi Arabia. The study was designed by obtaining a spectrum, that was analyzed, and was influenced by many parameters, including chemical characteristics of each metabolite and the compounds in which they are located; N-acetyl aspartate (NAA) , choline (Cho), creatine (Cr) Cho/ NAA, Cho/ Cr, NAA/ Cr , Lactate and Lipid at the selection of the lesion area to be studied. The perfusion MRI (rCBV) was characterized as normal, hyper, and hypo-perfused. Choice of the technique type to be employed was (PRESS and STEAM) and the choice of the echo time was (short and long). The diagnostic strategy was evaluated based on results of imaging of 128 patients who had completed data including age, tumor tertiary in the brain. Conventional MRI with standard diagnostic criteria, findings and application of scan with T1:TR<500ms and TE <50ms and T2 :TR>1500 and TE>80ms were obtained. MRI with contrast enhancement in T1 weighted image and nullify the signal from CSF were also been achieved . Adequate scan was attained with Short echo times (TEs) less than 30ms for STEAM and TE as long as 144ms and 288ms milliseconds for PRESS technique. For MRS long TE (1500/144ms) was used; for identification (Cho), (Cr), (NAA), and lactate.

Conversely, short TE (2000/35ms) was applied for identification of Lipids, lactate, ALA, myoinositol, glutamate, and glutamine.

The current study showed that the most common affected age was age between 41-50 years old constituting 34(26.6%). Distribution of tumor territory in the brain site has significant relation with age at *p*-value = 0.006.The entire lesions were diagnosed according to the standard criteria of diagnosis done by radiologist.

Astrocytomas, were found in 58(45.3%) of the cases, Gliomatosis Cerebri, Glioblastic Multiform (GBM) and Oligodendroglioma were 44 (34.4%) ,where the Lymphoma and Meningioma were found in 2(1.6%) and 8(6.3%) of the cases in respectively , where the metastases constituting 3(2.3%).Ependymal tumors were found to be 13(10.1%) 5 cases were Ependymoma and 8 were Subependymoma.

Significant results between the perfusion findings and the MRS values regarding Cho/ NAA at p= (0.000) and Cho/ Cr at p = (.000).Astrocytomas showed a relative reduction in NAA and Cr, and Cho comparing with the lymphoma .The spectra of metastases are similar to those of meningioma and gliomatos cerebri and ependemal tumors, with low NAA, low Cr, and high Cho levels. The difference was found to be significant in the NAA values at different brain lesions with no significant reduction or increasing in Cho and Cr. Cho/Cr has significant impact in differentiation of lymphoma from other lesions at p value = 0.004 where the other parameters including Cho/ NAA, NAA/ Cr, Lactate and Lipid showed no significant relations. By combining both MRS and perfusion MRI, the diagnosis of lesions was achieved with value of 0.94±.89 for NAA and Cho/ NAA 1.83±1.22.

A significant relation was found between the diagnosis and tumor character in Perfusion-MRI (rCBV) as normal, hypo-perfused and hyper- perfused at p-value=0.001 as well; the STEAM and PRESS results at P-value = 0.042 and 0.042 in respectively. Perfusion-MRI (rCBV) and MRS are useful for establishing the differential diagnosis between brain metastases and brain tumors.

Both has significant relation in differentiation and diagnosis of brain tumors regarding its perfusion as well in chemical characteristics of each metabolite and the compounds in which they are located; N-acetyl aspartate (NAA) , Cho/ NAA, Cho/ Cr at the selection of the area to study. So the combination of MRS and perfusion-weighted imaging may improve characterization of brain lesions.

NAA, Cho, Cr, NAA/ Cr, Lactate and Lipids metabolic values showed no significant relation between the values to be increased or decreased according to grading therefore the dependency of grading should be based upon the Cho/ NAA and Cho/ Cr .From this account and metabolic ratios; the study suggested to diagnose, differentiate and grade gliomas after evaluating the Cho/ NAA and Cho/ Cr.

Conclusion :MRS metabolic ratios (Cho/Cr and Cho/NAA) can be used to grade and differentiate gliomas. Ratios less than 1.5 were suggested to be considered as normal values, ratios from 1.5 to 2 were suggested to subsist as low grade glioma and ratios higher than 2 were suggested to be high grade glioma or metastasis. Meningioma can be diagnosed by conventional MRI images. MRS should be added to routine MR imaging studies as it provides greater information concerning tissue characterization than what is possible with MR imaging studies alone.

المستخلص

كان الهدف من هذه الدراسة تقييم فعالية التصوير بالرنين المغناطيسي التقليدي والتحليل الطيفي والوزن الأروائي في وصف أورام الدماغ. وقد أجريت الدراسة خلال الفترة التي امتدت من عام 2014 حتى عام 2017، باستخدام نظام "التصوير بالرنين المغناطيسي سينجو" المغناطيسية فائقة التوصيل 1.5 تسلا في قسم جراحة الاعصاب والأورام في منطقة جازان–المملكة العربية السعودية. صممت الدراسة بالحصول علي الطيف، ومن ثم تحليلها، وتأثره بالكثير من العوامل، بما في ذلك الخصائص الكيميائية لكل مستقلب والمركبات التي توجد فيها مثل NAA و Cho و Cr ، لاكتات والدهون في المنطقة المختارة من الورم لدراستها. واتسم الارواء بالعادي والمفرط والمقصر (Perfused) و اختيار نوع التقنية التي ستستخدم في الوقت القصير والطويل. وتم تقييم استراتيجية التشخيص استناداً إلى نتائج التصوير الذي تم علي 128 من المرضى الذين أكملوا البيانات بما في ذلك العمر ونوع الورم في منطقة الدماغ. التصوير بالرنين المغناطيسي التقليدي مع المعايير التشخيصية الرصينة، والتصوير بالرنين المغناطيسي مع استخدام وسيط التباين في مرحلة T1.

وأظهرت الدراسة الحالية أن السن الأكثر شيوعاً السن بين 41–50 سنة التي تشكل 34(26.6%). لمواقع الورم بالدماغ وكان له علاقة كبيرة بعمر المريض وتم تشخيص المرضي طبقاً للمعايير القياسية ووفقا للتشخيص الذي قام به أخصائي الأشعة ، في 58(45.3%) من الحالات للورم الدبغي (GBM) أوليجودينـدروجليوما 44 (34.4 في المائـة)، وسرطان الغدد الليمفاوية، والسحايا في 2(1.6%) و 8(6.3%) من الحالات على التوالي. وأظهرت الدراسة أن للمطياف المغنطيسي له دور محدود في تحسن الحالة الصحية للمرضى الذين يعانون أورام المخ الدبغي. الا أن استخدام المطياف المغنطيسي مع وجود جهاز الرنين المغنطيسي والوزن الأروائي والمعلومات السريرية الأولية يساعد في تشخيص بعض الأمراض والخلل الوظيفي. يمكن أن يستخدم المطياف المغنطيسي كأداة فعالة لتمييز أورام الدماغ المنخفضة والمرتفعة بالإضافة التمييز بين السرطان المنتكس وأمراض الدماغ الناتجة من استخدام العلاج الذري.

List of Contents

Items	Title	Page No
الآية		I
Dedication		II
Acknowledgement		III
Abstract		IV
المستخلص		V
List of tables		**X**
List of figures		**XI**
List of abbreviations		**XIII**
List of contents		**XIV**
Chapter one		
1. Introduction		**1**
1.1 Prelude		**2**
1.2 Problem Statement		**3**
1.3 objectives of the study		**4**
1.3.1 General objectives		**4**
1.3.2 Specific Objectives		**5**

Chapter two -Literature Review	
2. Anatomy of the brain	**6**
2.2 Brain meninges	**7**
2.3 Central and Peripheral Nervous Systems	**8**
2.1.3 Brain components	**11**
2.1.4 ventricular anatomy	**14**
2.1.6 circle of Willis	**16**
2.1.7 Cell types of the brain	**18**
2. Brain physiology	**21**
2.1.8 lobes of the brain	**21**
2.1.9 Ventricles and cerebrospinal fluid	**22**
2.1.10 basal ganglia	**23**
2.3 Brain pathology	**25**
2.3.1 WHO tumor grading system for adult brain tumor	**26**
2.3.2 Types of tumors	**27**
2.3.2.1Meningioma	**27**
2.3.2.2 Acoustic neuroma	**27**
2.3.2.3 Astrocytoma	**27**

2.3.2.4 symptoms of brain tumor	**27**
2.4.3 physical basis of MRS	**31**
2.4.4 tetra methyl silane (TMS)	**32**
2 previous studies	**36**
3.1 materials	**56**
3.1.2 Inclusion criteria	**57**
3.1,3 Exclusion criteria	**57**
3.2.1 Methods	**57**
3.2.2 MRI brain protocol	**59**
3.2.2.1 scout images (localizer)	**59**
3.2.2.2 reporting brain tumor	**61**
3.2.2.3 MRS Techniques	**62**
3.2.2.4 single voxel spectroscopy	**62**
3.2.2.5 special sequences	**63**
Chapter four Results	
4.1 Results	**69**

Chapter five **Discussion, Conclusion and Recommendation**	
5.1 Discussion	**81**
5.2 Conclusion	**92**
5.3 Recommendation	**94**
Appendices	
References	

List of tables

Table	Item	Page No
2-1	Summary neuron Types	**19**
3.1	Difference between single voxel and multi- voxel	**62**
4.1	Descriptive Statistics of classification of lesions according to WHO grading, MRS metabolite and Radiologist MR imaging features of brain tumors**.**	**73** **75**
4.2	Distribution of study sample according to radiologist diagnosis	**79**
4.3	Mean age, gender distribution, metabolite ratio values, diagnosis-category of grading tumors {mean values} and radiologist diagnosis according to the standard criteria of Pilocystic, Anaplastic and Diffused Astrocytoma.	**74** **77**
4.4	Mean age, gender distribution, Metabolite ratio Values, diagnosis-category of Grading tumors {mean values} and radiologist diagnosis according to the standard criteria of ependimal Tumors	**78**
4.5	Mean age, gender distribution, Metabolite Values, diagnosis-category of Grading tumors {mean values} and radiologist diagnosis according to the standard criteria of Glioblastic Multiform (GBM) Gliomatosis Cerebri and Oligodendroglioma	**79**
4.6	Mean age, gender distribution, Metabolite Values, diagnosis-category of Grading tumors {mean values} and radiologist diagnosis according to the standard criteria of Meningioma, Lymphoma	**79**
4.7	Metabolite Values, diagnosis-category of Grading tumors {mean values} and p- value	**79**

List of Figures

Figure	Items	Page No
Fig. 2-2	Protected layer bones of the skull and the vertebral column	**7**
Fig. 2-3	Compartments of the brain for body functions	**8**
Fig. 2-4	Brain MRI.T2- weighted, axial plain	**9**
Fig. 2-5	Brain MRI.T2- weighted, coronal plain	**10**
Fig. 2-6	Top: Superior view of the brain. Bottom: Inferior view of the brain	**12**
Fig. 2-7	Names of folding area of the cortex increases the brain's surface	**13**
Fig. 2-8	Ventricles Anatomy	**14**
Fig. 2-9	Brain blood supply	**15**
Fig. 2-10	Magnetic Resonance Angiography (MRA)	**16**
Fig. 2-11	Circle of Willis	**17**
Fig. 2-12	Microscopic view of neurons and glia cells	**18**
Fig. 2-13	The shape of the neuron	**17**
Fig. 2-14	The relationship of afferent and efferent	**20**
Fig. 2-15	The classification of neurons	**20**
Fig. 2-16	Lobes of the Cerebral Cortex	**21**
Fig. 2-17	Lobes of the Cerebral Cortex	**22**
Fig. 2-18	Lobes of the Cerebral Cortex	**23**
Fig. 2-19	Sagittal MRI views of the brain	**24**
Fig. 2-20	Sites of tumors in the human brain	**25**
Fig. 2-21	Tumor press the function unit of brain (neurons)	**28**
Fig. 2-22	Intracranial tumors that reflect the clinical manifestation	**28**
Fig. 2-23	3D MRI showing the invasion and compression	**29**
Fig. 2-24	Intracranial tumors that reflect the clinical manifestation	**29**
Fig. 2-25	Compression of tumor to normal cells and causing deficit to normal function	**30**
Fig. 2-26	Tumor surrounded by fluid due to the irritation of normal cells	**30**
Fig. 2-27	Protons of (TMS) are highly shielded	**32**
Fig. 2-29	Single voxel in MRI	**35**

Fig. 2-30	Single voxel for comparison	**36**
Fig. 2-31	Difference between single voxel and multi- voxel	**37**
Fig. 2-32	Multi-voxel scan	**38**
Fig. 2-33	MRS Short TE	**39**
Fig. 2-34	MRS long TE	**40**
Fig. 2-35	MR spectroscopy of the right temporal lesion	**40**
Fig. 2-36	A good quality spectrum	**41**
Fig. 2-38	MR spectroscopy of the right temporal lesion	**68**
Fig. 2-39	Gliomatosis cerebri with elevated choline and reduced lipid	**69**
Fig. 2-40	Primary CNS lymphoma with elevated choline reduced NAA	**70**
Fig. 2-41	MRS with elevated Cho/NAA in lesion	**71**

List of Abbreviations

ACC:	Anterior Cingulate Cortex
BG:	Basal Ganglia
BOLD:	Blood-Oxygen Level Dependent functional MRI
C ho:	Choline
Cr:	Creatine
CSI :	Chemical-Shift Imaging (It is technique, which is used for the measurement of chemicals)
DQF:	Double-Quantum Filtered
FRO:	Frontal
GABA:	C-Amino Butyric Acid
GABA-T:	GABA Transaminase
GAD:	Glutamic Acid Decarboxylase
GAT:	GABA Transporters
Gln:	Glutamine
Glu:	Glutamate + Glutamine
HIPPO **:**	Hippocampal Area
IGE:	Idiopathic Generalized Epilepsy
MEGA - PRESS:	J-Difference Edited PRESS
MP:	MEGA-PRESS
MR:	Magnetic Resonance

MRSI:	Magnetic Resonance Spectroscopic Imaging
NAA:	N-Acetyl Aspartate
NMR:	Nuclear Magnetic Resonance
PRESS:	Point-Resolved Spectroscopy (A very common screening approach)
SAD:	Social Anxiety Disorder
SE:	Spin Echo (It is the refocusing of magnetism related to MRI)
SM:	sensorimotor
SN:	Substantia Nigra
SNR:	Signal-To-Noise Ratio
SSRI:	selective serotonin reuptake inhibitor
STEAM:	Stimulated-Echo Acquisition Mode (STEAM is a spectroscopy method used for screening)
SVS:	Single Voxel Spectroscopy (An screening technique)
TE:	Echo Time
Th:	Thalamus

Chapter One
Introduction

Chapter one
Introduction

1.1 Prelude

Brain tumors can be defined as the development of abnormal cells within different parts of the brain. Brain tumors usually develop, when the tumors cells escape from the normal physiological control and invade nearby healthy cells. Any healthy cerebral cell, membrane, or covering of brain can be converted into benign or malignant tumor. There are various types of brain tumors, which have their own symptoms and complications. The two major types of brain tumors include benign tumors and malignant tumors. Moreover, malignant brain tumors are further divided into two categories that include primary tumors and secondary tumors. **(*Tony Talebei, et al 2017)***

Gliomas are considered as the most primary type of brain tumors. These types of tumors are divided into various categories according to their aggressiveness and morphology. This type of tumor always originates from glial cells, which include astrocytes and oligodentrocytes. The nature of Gliomas is infiltrative, which has the capability to result in neuronal cell damage and decreased N-acetyl aspartate (NAA). The actual cause of this tumor is still unknown; however, presence of genetic disorders is the leading cause for the occurrence of gliomas**. *(Andreasen NC ,1988)***

It is extremely difficult for the health care professionals to make a strong prognosis of malignant gliomas. The reason is that malignant glioma has increased relapse rate and infiltration nature. Therefore, the therapeutic approaches are always different for every different type of the tumor.(***Henry R.G ,et al 2002***)

There are various in vivo approaches, which are used in the clinical settings for the determination of tumor grade and appropriate treatment.

The use of conventional magnetic resonance imaging with contrast media makes positive effects in the process of characterization. However, detection of malignancy does not require any area of contrast media enhancement. (***Pandey, R. J., et al 1995***)

The reason behind this statement is that some low-grade tumors have shown contrast enhancement; whereas, few glioblastomas have not shown any contrast enhancement. Therefore, high and low grade brain tumors cannot be distinguished with the help of contrast enhancement consistently. Inappropriate signals around tumors on T2-weightes images will be non-specific, since they can represent vasogenic edema, neoplastic infiltration, or both. The data, which is derived out by diffusion weighted imaging, MRS, and perfusions are totally dependent upon one another**.** However, all of these approaches are complementary to magnetic resonance imaging**.**

(Law, M. C.,et al, 2002)

The approach of MR spectroscopy along with single voxel is considered as the significant method for the determination of gliomas. However, it will be difficult to evaluate the spatial distribution of spectral alterations. Modern developments and investigations in MR spectroscopy have resulted in the attainment of chemical shift imaging (CSI) with increased spatial resolution. Almost every imaging modality has the ability of detecting brain tumors selectively as non-invasive technique.

Furthermore, conventional CT and MRI are also used in the clinical settings to detect tumors of brains. However, MRA, CTA, functional MRI, PET/CT, and PET/MRI are also used for differential diagnosis. For accurate and final diagnosis, histopathology (invasive technique) is widely used in the hospital settings with the guides of MRS to correct area.***(Graves, E. N., et al, 2001)***

Diagnosing, staging, and re-staging of cancer, as well as the planning and monitoring of cancer treatment, have traditionally relied heavily on anatomic imaging with computed tomography (CT) or magnetic resonance imaging modalities (MRI).

These anatomic imaging modalities provide exquisite anatomic detail and are invaluable, especially for guiding surgical intervention and radiotherapy. However, they do have limitations in their ability to characterize tissue reliably as malignant or benign. Anatomic imaging generally has a high sensitivity for the detection of obvious structural alteration (e.g. enlarged structures, abnormal imaging characteristics) but a low specificity for further characterizing these abnormalities as malignant or benign. Necrotic tissue, scar tissue, and inflammatory changes often cannot be differentiated from malignancy based on anatomic imaging alone. ***(Barker, P. L.,et al 1995)***

1.2 Problem Statement

Since brain acts as a master of human organs, and plays a major role for controlling, coordinating, and organizing most human activities and personality. Brain tumors can disturb biological, physiological, and chemical activities of the organ. Therefore, proper diagnosis is extremely necessary for delivering quality healthcare to the patients.

For the purpose of diagnosis, numerous imaging modalities are presently used in radiology practice for the detection of brain tumors.

It is a fact that imaging modalities, which are being used for brain tumors, are usually selective, but not specific. Therefore, specific method is extremely important to be used for proper diagnosis of brain tumors. For accurate and final diagnosis, the approach of tumor biopsy is widely used in the health care organizations. It is an invasive technique, which can be dangerous for brain substances and can lead the patient towards certain deficits on temporary or permanently basis***.(Lin DD, Crawford TO, Barker PB ,2003)***

The questions to be answered

1. Can MRS replace biopsy ?
2. What are the diagnostic performance of MRI,MRS and Perfusion technique in the diagnosis of brain tumors?
3. Is apparently viable tumor well-defined in MRI?
4. Can the grading of the tumors done by the MRS?

1.3 objectives of the study

1.3.1 General objectives:

To study the Diagnostic Performance of MRI, MRS and Perfusion weighted in Characterization of Brain Tumors

1.3.2 Specific Objectives

- To characterize the brain lesions in perfusion (as hypo- normal –hyper) perfusion.
- To characterize the brain lesions in short and long echo time (TE).
- To evaluate the metabolite N-acetyl aspartate (NAA) , choline (Cho), creatine (Cr) Cho/ NAA, Cho/ Cr, NAA/ Cr , Lactate and Lipid at the selection of the lesion area to be studied.
- To evaluate the common site of the lesion.
- To correlate the metabolite values with the final diagnosis of brain
- To characterize the brain tumor type according to refers characteristics
- To correlate the grading of the tumor to the metabolite values
- To correlate the metabolite value with results of reference ,STEAM and PRESS

Chapter Two
Literature Review

Chapter Two

Literature Review

2. Anatomy of the brain

2.1 Overview:

The human brain is an amazing three- pound organ that controls all functions of the body, interprets information from the outside world, and embodies the essence of the mind and soul. Intelligence, creativity, emotion, and memory are a few of the many things governed by the brain. Protected within the skull, the brain is composed of the cerebrum, cerebellum, and brainstem.

The brainstem acts as a relay center connecting the cerebrum and cerebellum to the spinal cord. (***Snell, Richard S, 2010***)

Human brain is divided to compartments; every compartment responsible for specific task for motor and sense activity as shown in figure below. Any trauma, infection or tumors can alter the physiology and anatomy of the brain which can be detected as functional deficit when clinical exam done for the assessment of brain activity. Sight, smell, touch, taste, and hearing- often many at one time. It assembles the messages in a way that has meaning for us, and can store that information in our memory. The brain controls our thoughts, memory and speech, movement of the arms and legs, and the function of many organs within our body. It also determines how we respond to stressful situations such as taking a test, losing a job, or suffering an (illness) by regulating our heart and breathing rate. (***Snell, Richard S, 2010)***

2.2 Brain meninges

The meninges are three layers of protective tissue called the dura mater, arachnoid mater, and pia mater that surround the neuraxis. The meninges of the brain and spinal cord are continuous, being linked through the magnum foramen. ***(Tamraz et al ,2000)***

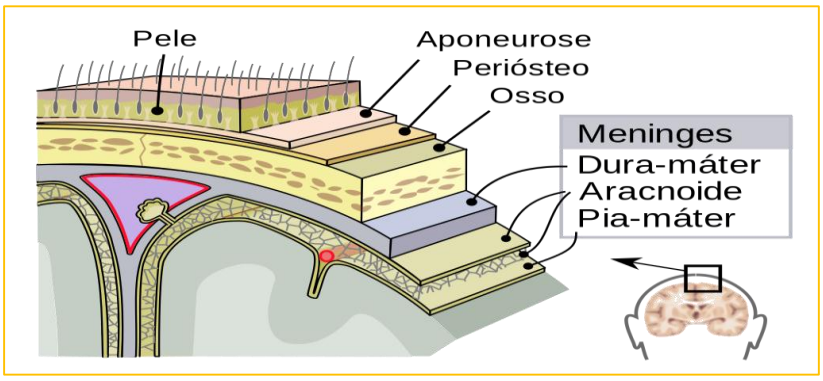

Figure: 2-1(A) *: Shows the meninges of the central nervous system which include: Dura matter, arachnoid and pia matter as shown in the picture.* ***(Tamraz,et al,2000)***

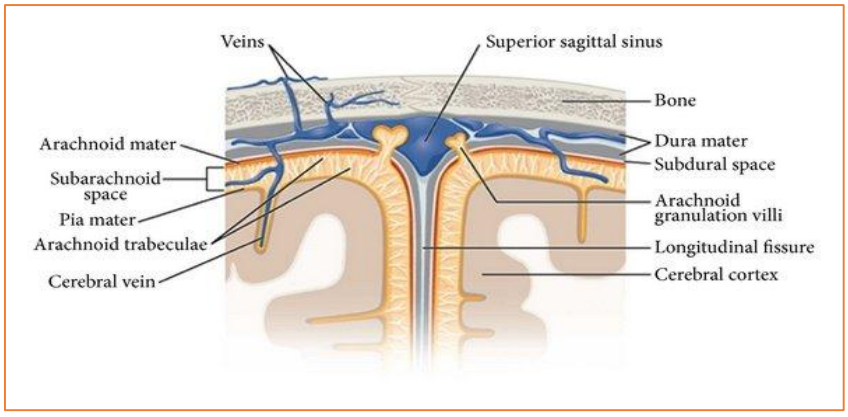

Figure 2-1(B) ***Shows in detail the layers of meninges and venous system of meninges****(Tamraz,et al 2000)*

2.3 Central and Peripheral Nervous Systems

The nervous system is divided into two main parts, for purposes of description: the central nervous system (Figure. 2-B), which consists of the brain and spinal cord. Both the brain and spinal cord are covered with a system of membranes, called meninges, and are suspended in the cerebrospinal fluid; they are further protected by the bones of the skull and the vertebral column (Figure. 2-A).
The central nervous system is composed of large numbers of excitable nerve cells and their processes, called neurons, which are supported by specialized tissue called neuroglia. The long processes of a nerve cell are called axons or nerve fibers. The interior of the central nervous system is organized into gray and white matter. Gray matter consists of nerve cells embedded in neuroglia; it has a gray color. White matter consists of nerve fibers embedded in neuroglia; it has a white color due to the presence of lipid material in the myelin sheaths of many of the nerve fibers. ***(Tamraz et al ,2000)***

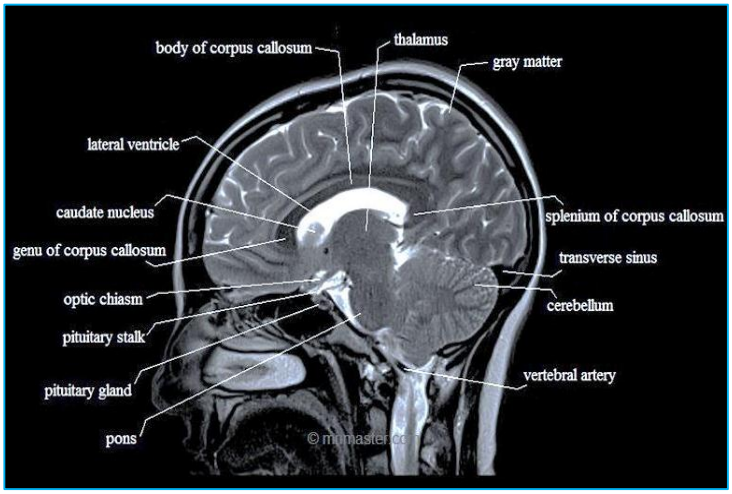

(*Figure: 2-2(A) Brain anatomy of MRI T2 sagittal view showing internal components of cerebrum and its relationship with CSF (Tamraz et al ,2000)*

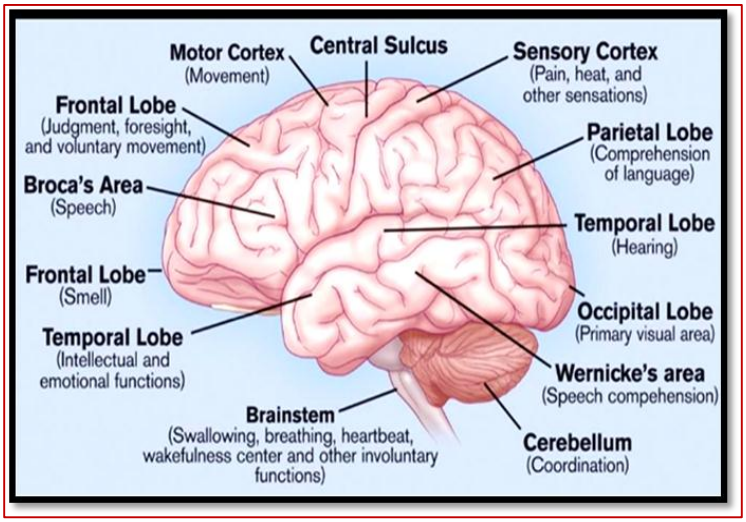

Figure (2-3)

Figure (2-3) Shows the compartments of the brain for body functions and controlled by just 1 part of the brain. Other functions are controlled by more than 1 part

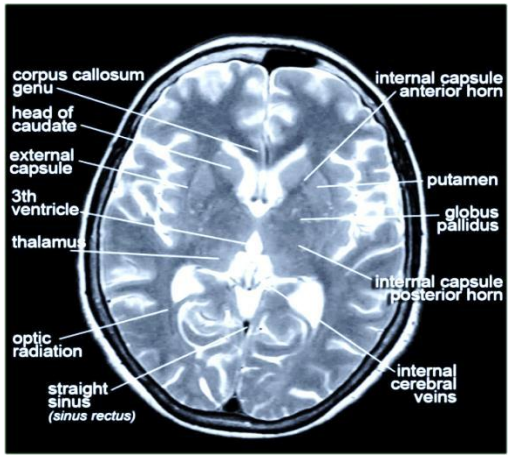

Figure (2-3)

Brain anatomy MRI T_2 axial view at the level of basal ganglia (Tamraz,et al,2000)

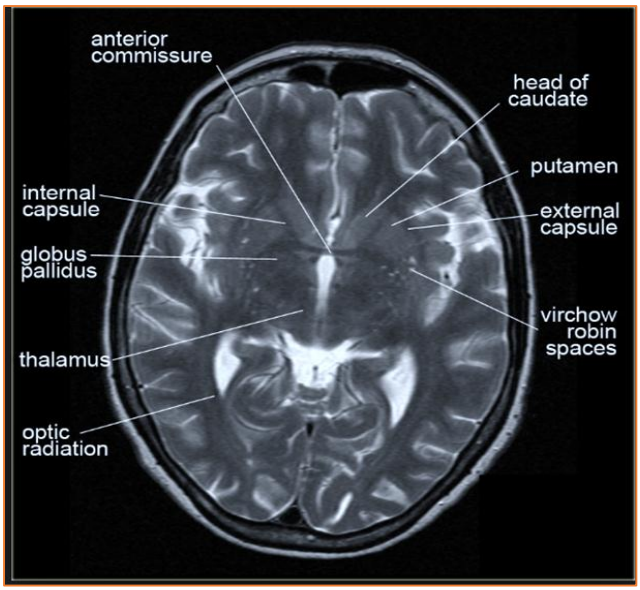

Figure (2-4) Brain MRI.T2- weighted, axial plain through level of internal and external capsule showing thalamus, anterior commissure (Tamraz,et al 2000)

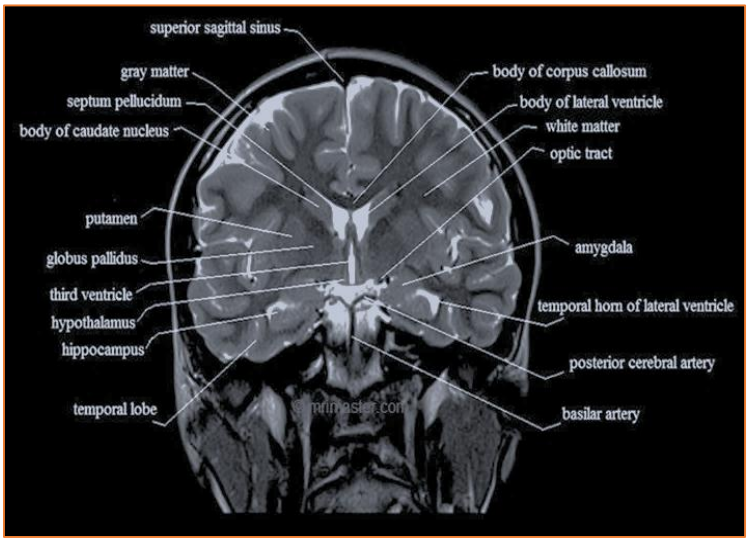

Figure (2- 5) Brain MRI.T2- weighted, coronal plain through level of internal and external capsule showing amygdala , hippocampus and third ventricle (Tamraz,et al,2000)

2.1.3 Brain components

The brain is composed of the cerebrum, cerebellum, and brainstem Figure (6). Cerebrum is the largest part of the brain and is composed of right and left hemispheres. It performs higher functions like interpreting touch, vision and hearing, as well as speech, reasoning, emotions, learning, and fine control of movement. Cerebellum is located under the cerebrum. Its function is to coordinate muscle movements, maintain posture, and balance.

Brainstem includes the midbrain, pons, and medulla. It acts as a relay center connecting the cerebrum and cerebellum to the spinal cord. It performs many automatic functions such as breathing, heart rate, body temperature, wake and sleep cycles, digestion, sneezing, coughing, vomiting, and swallowing. Ten of the twelve cranial nerves originate in the brainstem. The surface of the cerebrum has a folded appearance called the cortex. The cortex contains about 70% of the 100 billion nerve cells. The nerve cell bodies color the cortex grey- brown giving it its name gray matter

Beneath the cortex are long connecting fibers between neurons, called axons, which make up the white matter. The folding of the cortex increases the brain's surface area allowing more neurons to fit inside the skull and enabling higher functions. Each fold is called a gyrus, and each groove between folds is called a sulcus. There are names for the folds and grooves that help define specific brain regions. ***(Snell, Richard S. 2010)***

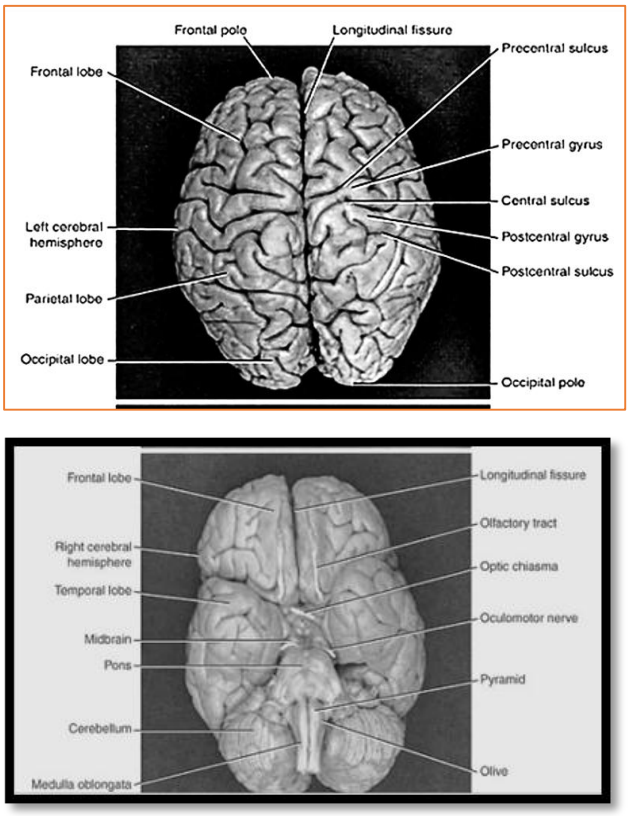

Figure (2-6) Top: Superior view of the brain.
Bottom: Inferior view of the brain
(Snell, Richard S. 2010)

Beneath the cortex are long connecting fibers between neurons, called axons, which make up the white matter. The folding of the cortex increases the brain's surface area allowing more neurons to fit inside the skull and enabling higher functions ***(Snell, Richard S. 2010)***

Brainstem includes the midbrain, pons, and medulla. (Figure 6) It acts as a relay center connecting the cerebrum and cerebellum to the spinal cord. It performs many automatic functions such as breathing, heart rate, body temperature, wake and sleep cycles, digestion, sneezing, coughing, vomiting, and swallowing.

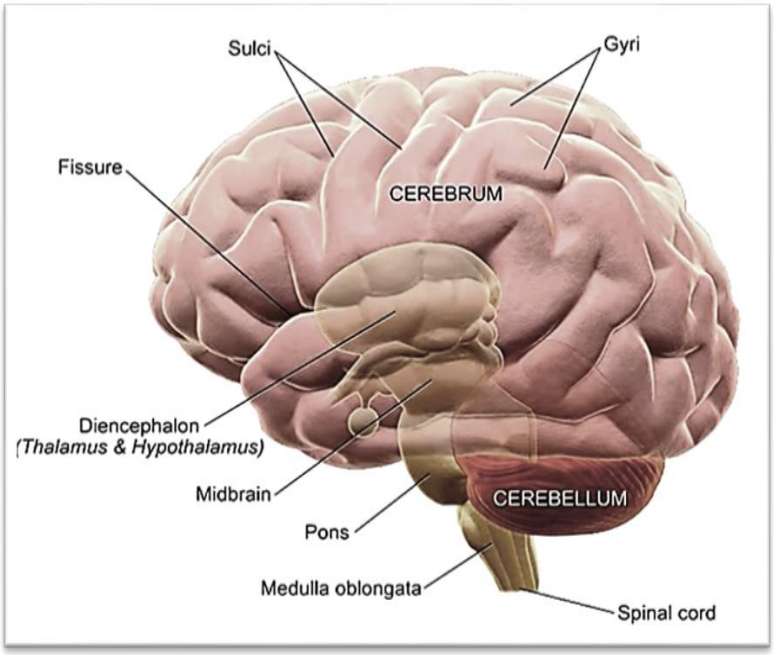

Figure(2-7)

Names of folding area of the cortex for example fissure, sulci, gyri and thalamus&hypothalamus (Snell, Richard S, 2010)

The folding of the cortex increases the brain's surface area allowing more neurons to fit inside the skull and enabling higher functions.

2.1.4 Ventricular Anatomy

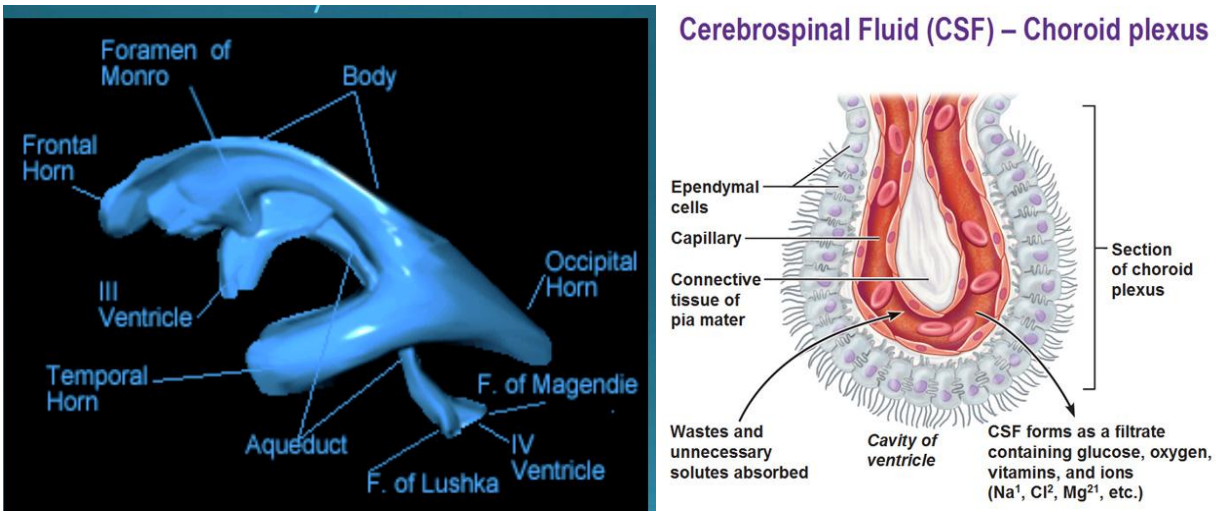

A *Figure (2-8)* B

A :Ventricular anatomy shows the shape and location of the each ventricle B: Microscopic anatomy of the origin of the cerebrospinal fluid in the choroid plexus (Snell, Richard S , 2010)

2.1.5 Brain blood supply

Blood is carried to the brain by two paired arteries, the internal carotid arteries and the vertebral arteries (Figure 23). The internal carotid arteries supply most of the cerebrum. The vertebral arteries supply the cerebellum, brainstem, and the underside of the cerebrum. After passing through the skull, the right and left vertebral arteries join together to form the basilar artery. The basilar artery and the internal carotid arteries "communicate" with each other at the base of the brain called the Circle of Willis

The communication between the internal carotid and vertebral basilar systems is an important safety feature of the brain. If one of the major vessels becomes blocked, it is possible for collateral blood flow to come across the Circle of Willis and prevent brain damage. The two systems connect at the circle of Willis.

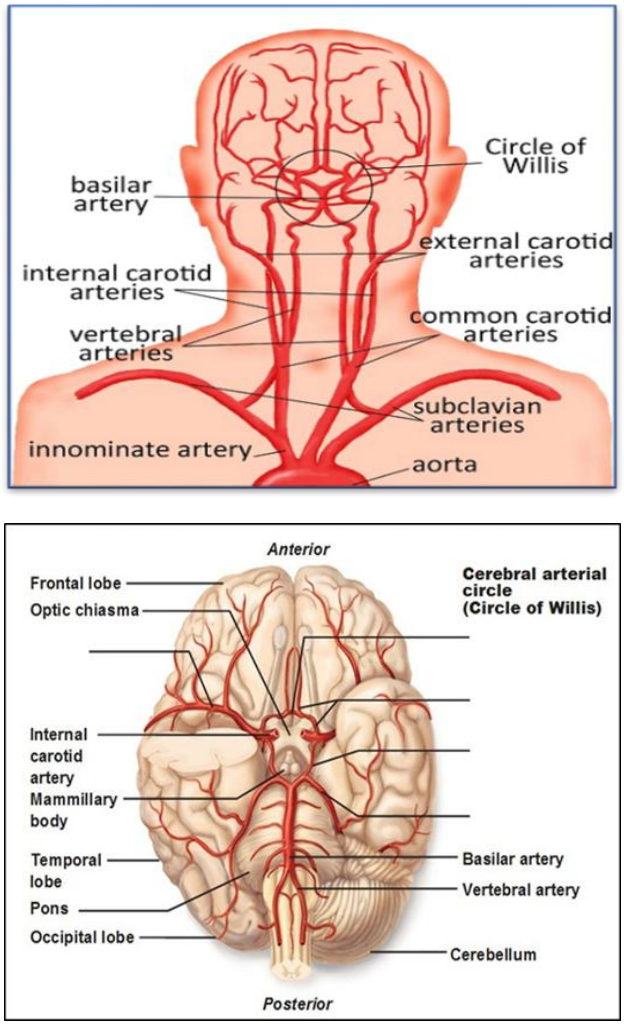

Figure (2-9)

A. Aortic arch supply the brain with the main oxygenated blood coronal view

B. Major arteries serving the brain (inferior view) (Snell, Richard S, 2010)

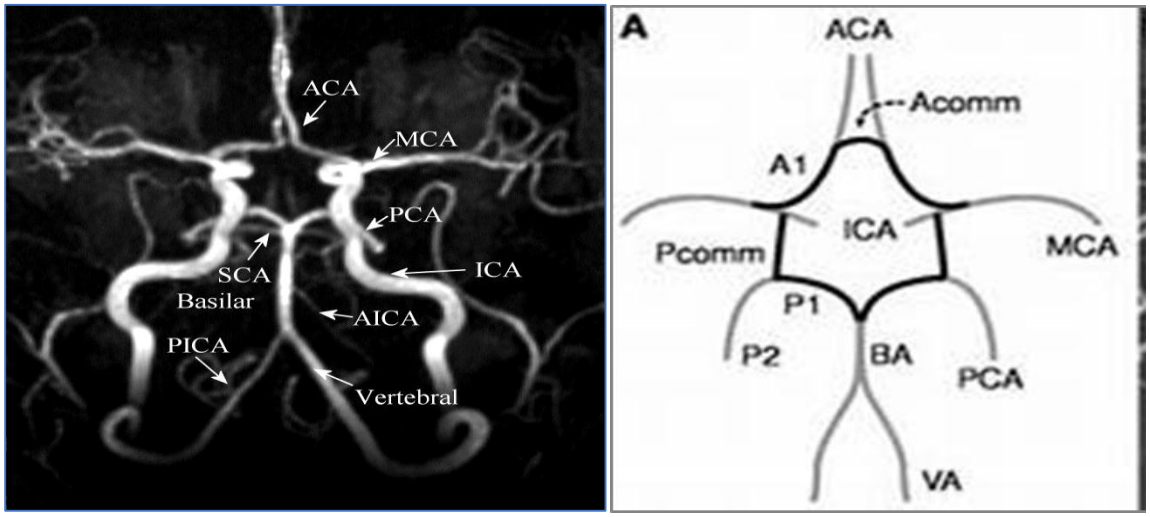

A Figure (2-10) B

Magnetic Resonance Angiography (MRA) Intracranial Study. ACA - anterior cerebral artery; MCA - middle cerebral artery; PCA - posterior cerebral artery; SCA - superior cerebellar artery; AICA - anterior inferior cerebellar artery; PICA - posterior inferior cerebellar artery (Tamraz,et al,2000)

2.1.6 The Circle of Willis

The importance of blood supply to the brain explains why there are so many pathways for oxygenated blood. As the internal carotid artery enters the head, it gives off a branch to one side called the anterior cerebral artery. This anterior cerebral artery will then connect to the anterior cerebral artery on the other side of the head and, therefore, by extension, to the internal carotid artery on the other side of the head as well. The posterior cerebral arteries will also connect to the internal carotid artery through a small vessel. This, therefore, completes a circle of connected arteries, located at the base of the brain, which supply the brain with blood, and call this structure called the Circle of Willis. Figure (2-14 A &B)

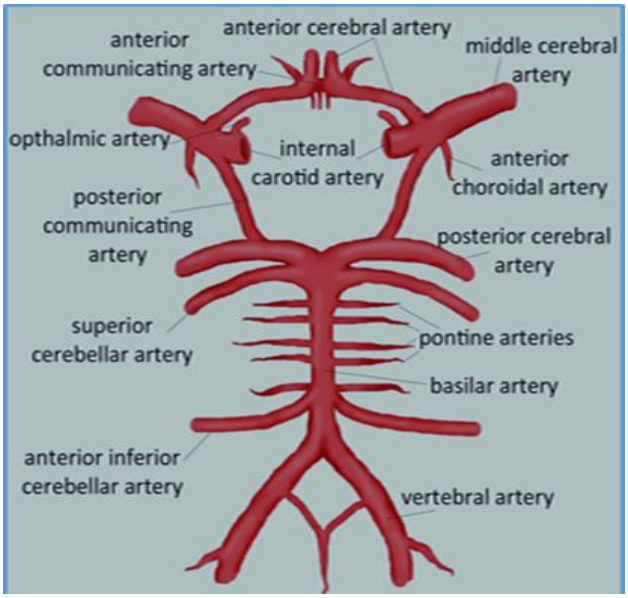

Figure (2-11A) Base of the skull

Circle of Willis illustrate the multi-branch of blood supply to the brain

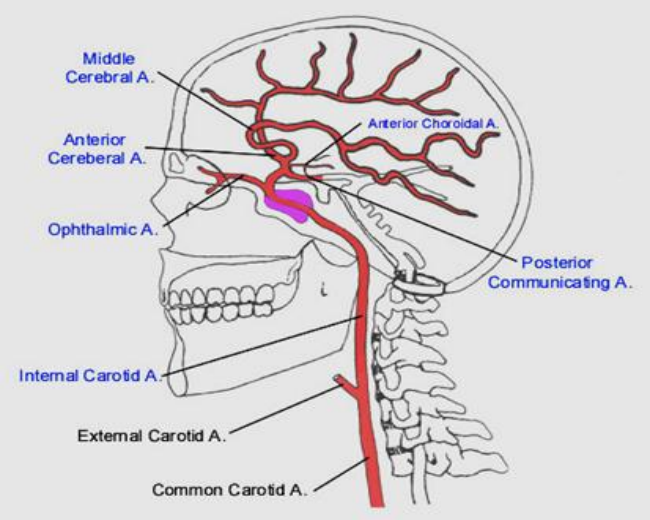

Figure (2-11B)
Lateral view of the skull showing the common carotid artery
Circle of Willis illustrate the multi-branch of blood supply to the brain
(Snell, Richard S, 2010)

2.1. 7 Cells types of the brain

The brain is made up of two types of cells: nerve cells (neurons) and glia cells. Neurons have two "processes" called axons and dendrites....glial cells have only one. Neurons can generate action potentials...glial cells cannot. However, glial cells do have a resting potential. Neurons have synapses that use neurotransmitters...glial cells do not have chemical synapses. ***(Snell, Richard S, 2010)***

It is also proposed that the basic functional unit in the brain is defined by how neurons communicate, and consists of two neurons and their interconnecting dendritic-synaptic-dendritic field. Since a functional unit is composed of two neurons, it requires two structural units to form a functional unit. (***Snell, Richard S, 2010)***

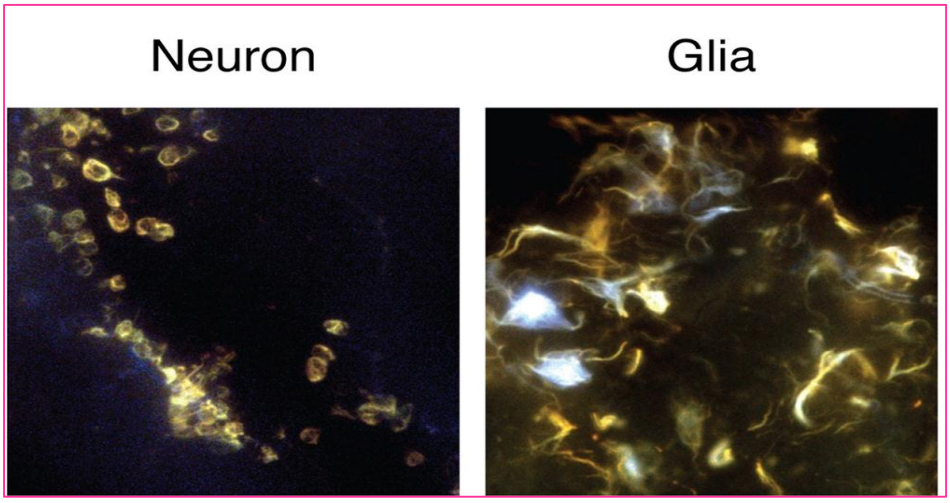

Neuron cells ***Figure (2-12)*** ***Glia cells***

Figure(2-12) shows the microscopic view of the main two types of the brain cells: neurons and glia cells (Snell, Richard S, 2010)

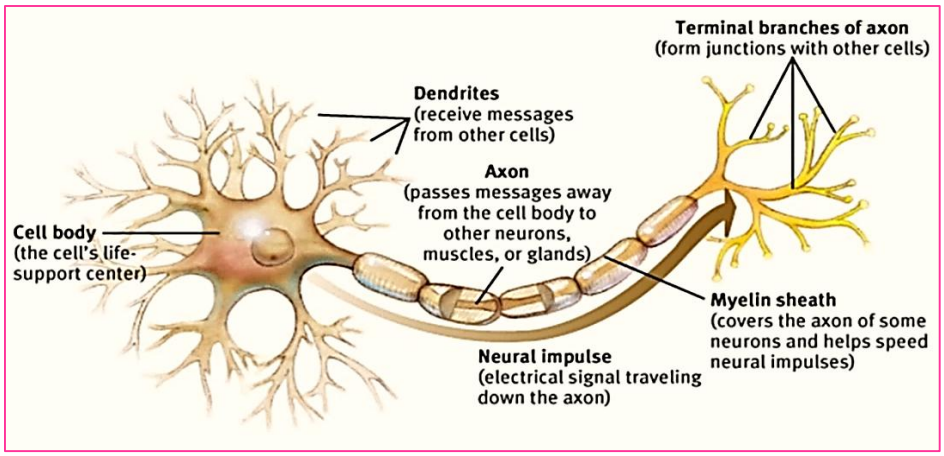

Figure (2-13)

The shape of the neuron (functional unit of the brain)
(Snell, Richard S, 2010)

Table 2-1 Summary neuron Types

	Sensory neurons	Interneurons	Motor neurons
Structure	Long dendrite Short axon	Short dendrite Short axon	Short dendrite Long axon
Function	Receive signals from environment and send impulses to the spinal cord and brain	Nerve that make up brain and spinal cord. Process impulses and send impulses to motor neurons	React to impulses from the brain and spinal cord (activate muscle and gland)
Location	Cell body /dendrite outside spinal cord Cell body- dorsal root	Entirely with in central nerve system (CNS)	Cell body /dendrite in spinal cord Axon outside spinal cord

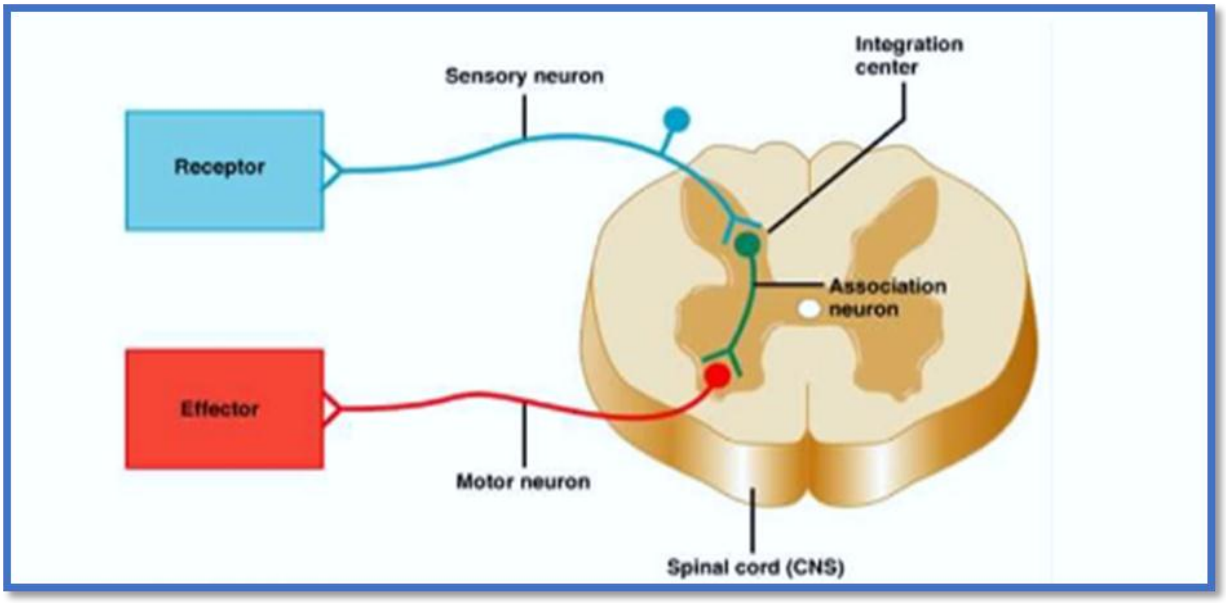

Figure (2-14)

The relationship of afferent sensory stimuli to memory bank, correlation and coordinating centers, and common efferent pathway (Snell, Richard S. 2010)

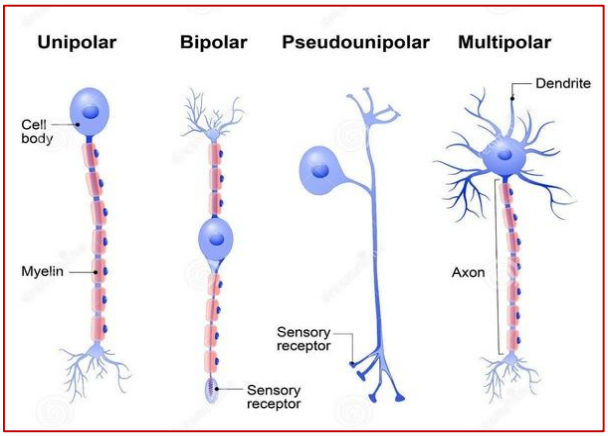

Figure (2-15)
The classification of neurons according to the number, length, and mode of branching of the neurites. (Snell, Richard S,2010)

Brain physiology

2.1.8 Lobes of the brain

The cerebral hemispheres have distinct fissures, which divide the brain into lobes. Each hemisphere has 4 lobes: frontal, temporal, parietal, and occipital (Figure 2-8)

Each lobe may be divided, once again, into areas that serve very specific functions. It's important to understand that each lobe of the brain does not function alone. There are very complex relationships between the lobes of the brain and between the right and left hemispheres**.** ***(Snell, Richard S, 2010)***

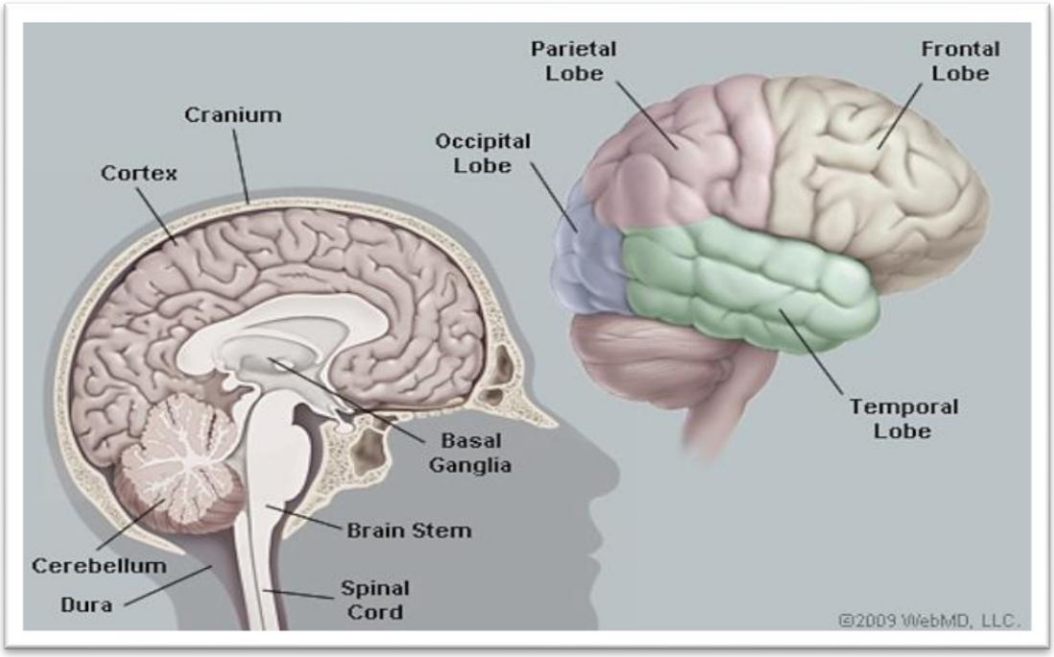

Figure (2-16) Lobes of the Cerebral Cortex
The division of cerebral cortex into four lobes. Extensive folding increases the surface area available for cerebral functions. (Snell, Richard S, 2010)

2.1.9 Ventricles and cerebrospinal fluid

The brain has hollow fluid filled cavities called ventricles (Figure.2-17). Inside the ventricles is a ribbon like structure called the choroid plexus that makes clear colorless cerebrospinal fluid (CSF). CSF flows within and around the brain and spinal cord to help cushion it from injury. ***(Snell, Richard S. 2010)***

This circulating fluid is constantly being absorbed and replenished.

There are two ventricles deep within the cerebral hemispheres called the lateral ventricles. They both connect with the third ventricle through a separate opening called the foramen of Monro. The third ventricle connects with the fourth ventricle through a long narrow tube called the aqueduct of Sylvius. ***(Snell, Richard S. 2010)***

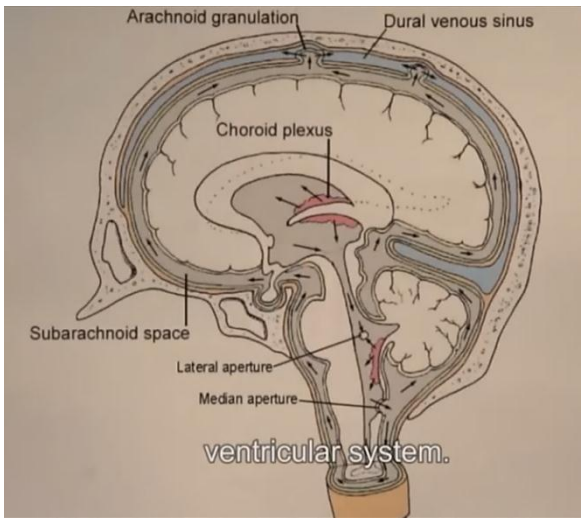

Figure (2-17)

Shows the two ventricles deep within the cerebral hemispheres called the lateral ventricles are connect with the third ventricle through a separate opening called the foramen of Monro. (Snell, Richard S. 2010)

2.1.10 Basal ganglia

Includes the caudate, putamen and globus pallidus (Figure 18A& B)These nuclei work with the cerebellum to coordinate fine motions, such as fingertip movements. They are strongly interconnected with the cerebral cortex, thalamus, and brainstem, as well as several other brain areas. The basal ganglia are associated with a variety of functions, including control of voluntary motor movements, procedural learning, habit learning, eye movements, cognition, and emotion. ***(Snell, Richard S. 2010)***

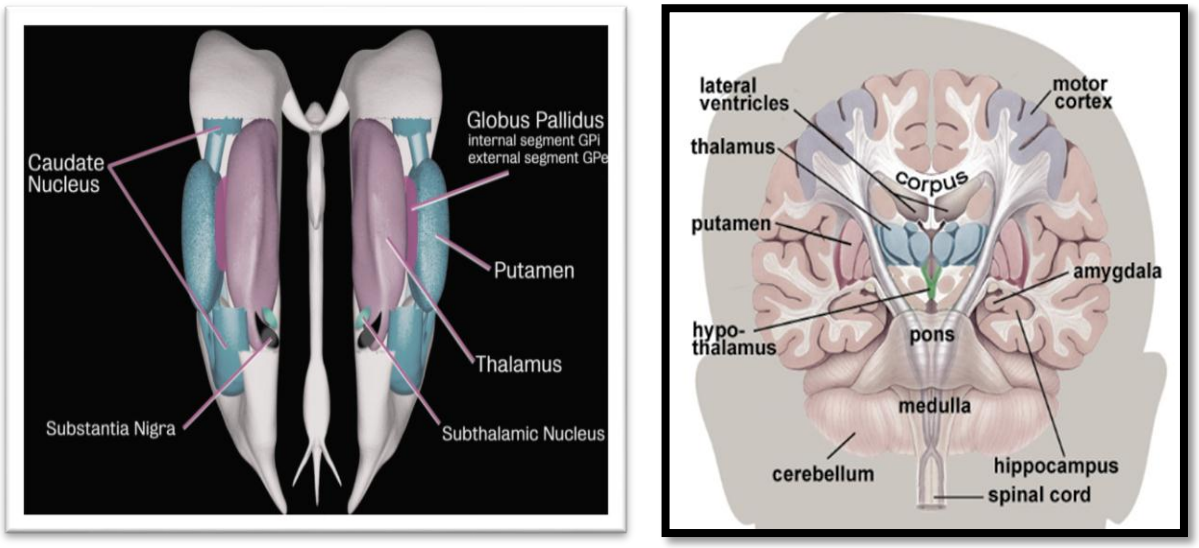

A B

Figure (2-18) A& B

Fig (2-10) A& B are showing the basal ganglia which associated with a variety of functions, including control of voluntary motor movements, procedural learning, habit learning, eye movements, cognition, and emotion

(Tamraz,et al ,2000)

From the fourth ventricle, CSF flows into the subarachnoid space where it bathes and cushions the brain. CSF is recycled (or absorbed) by special structures in the superior sagittal sinus called arachnoid villi. ***(Tamraz,et al2000)***

A balance is maintained between the amount of CSF that is absorbed and the amount that is produced. A disruption or blockage in the system can cause a buildup of CSF, which can cause enlargement of the ventricles (hydrocephalus) or cause a collection of fluid in the spinal cord (syringomyelia).

CSF fluid circulates inside the brain and spinal cord and then outside to the subarachnoid space. Hydrocephalus is cause a collection of fluid in the spinal cord (syringomyelia). CSF fluid circulates inside the brain and spinal cord and then outside to the subarachnoid space. ***(Tamraz,et al2000)***

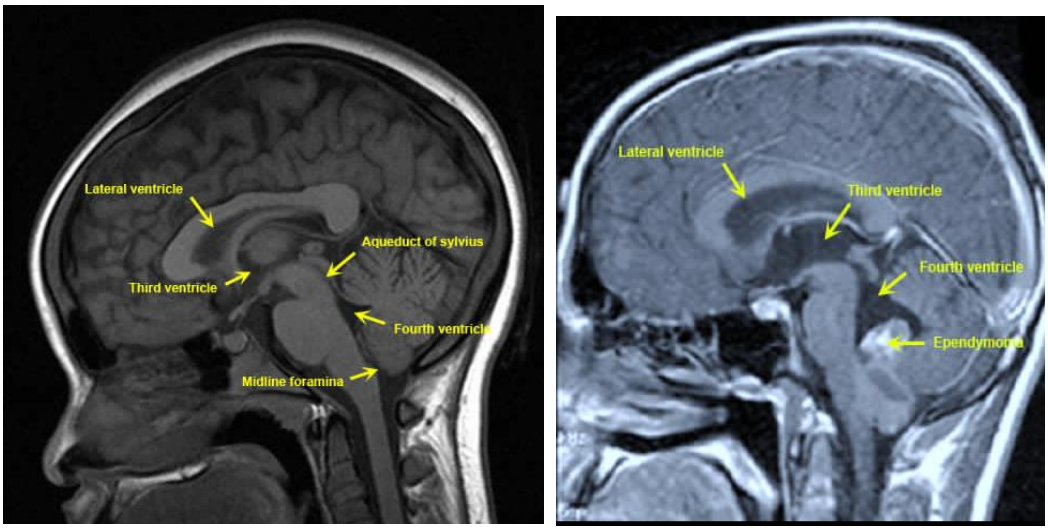

Figure (2-19)

Sagittal MRI views of the brain illustrate the course of CSF which cause a collection of fluid in the brain or spinal cord (Tamraz,et al2000)

2.3 Brain Pathology

A brain tumor occurs when abnormal cells form within the brain. There are two main types of tumors: malignant or cancerous tumors and benign tumors. Cancerous tumors can be divided into primary tumors that start within the brain, and secondary tumors that have spread from somewhere else, known as brain metastasis tumors. All types of brain tumors may produce symptoms that vary depending on the part of the brain involved. These symptoms may include headaches, seizures, problem with vision, vomiting, and mental changes. The headache is classically worse in the morning and goes away with vomiting. More specific problems may include difficulty in walking, speaking, and with sensation. As the disease progresses unconsciousness may occur. How quickly a brain tumor grows can vary greatly. The growth rate as well as location of a brain tumor determines how it will affect the function of your nervous system.
The following image illustrate the common sites of brain tumor as WHO**.**

(Dana, Faber, 2013)

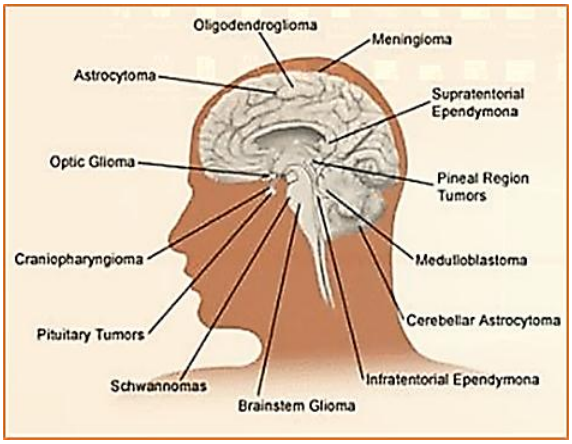

Figure (2-20) Sites of tumors in the human brain

(Andreasen N.C, et al 1988)

2.3.1 WHO tumor grading system for adult brain tumors

Brain tumors are named based on the type of cell they formed in, and where the tumor first formed in the central nervous system. While the extent or spread of most cancers is usually described in terms of stages, there is no standard staging system for brain and spinal cord tumors. A tumor is graded based on whether it is slow-growing or fast-growing.

The World Health Organization (WHO) grades tumors based on how the cancer cells look under a microscope and how quickly the tumor is likely to grow and spread. Brain tumors are categorized or graded on a scale of I to IV, with I being low-grade (slow-growing) and IV being high-grade (rapidly growing).

- **Grade I (low-grade)**: The tumor grows slowly, has cells that look a lot like normal cells, and rarely spreads into nearby tissues. Grade I brain tumors may be cured if they are completely removed by surgery.
- **Grade II**: The tumor grows slowly, but may spread into nearby tissue and may recur (come back). Some tumors may become a higher-grade tumor.
- **Grade III**: The tumor grows quickly, is likely to spread into nearby tissue, and the tumor cells look very different from normal cells.
- **Grade IV (high-grade)**: The tumor grows and spreads very quickly, and the cells do not look like normal cells. There may be areas of dead cells in the tumor. Grade IV tumors usually cannot be cured. ***((Dana, F., 2013)***

2.3.2 Types of Tumors

2.3.2.1 Meningioma: A meningioma is a tumor that arises from the membranes that surround your brain and spinal cord (meninges). Most meningioma are noncancerous.

2.3.2.2 Acoustic neuroma **(Schwannomas):** These are benign tumors that develop on the nerves that control balance and hearing leading from your inner ear to your brain.

2.3.2.3 Astrocytoma, Brain metastases, Choroid plexus carcinoma, Craniopharyngioma, Ependymoma , Glioblastoma and Glioma ***(Kleihues, B. W.,et al 1993)***

2.3.2.4 Symptoms of Brain Tumors

Headaches**,** seizures visual changes **,** changes in personality, mood, mental capacity and concentration , gastrointestinal symptoms such as nausea, loss of appetite, and vomiting .

Seizures are a presenting symptom in in approximately 20%of patients

Among all patients with brain tumors, 70% with primary tumors and 40% with metastatic brain tumors develop seizures at some time during the clinical course.

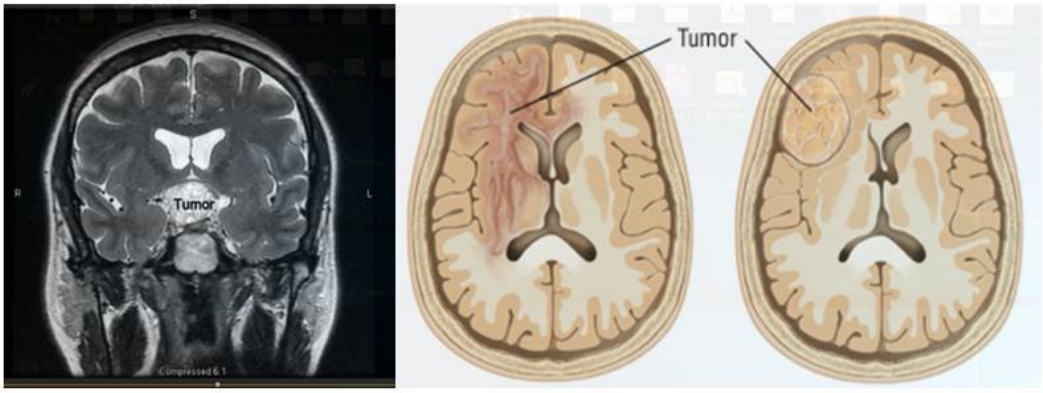

A ***B*** ***C***

Figure (2-21)

Tumor press the function unit of brain (neurons) and causes seizures visual changes in most of the tumors. (Andreasen N.C., et al, 1988)

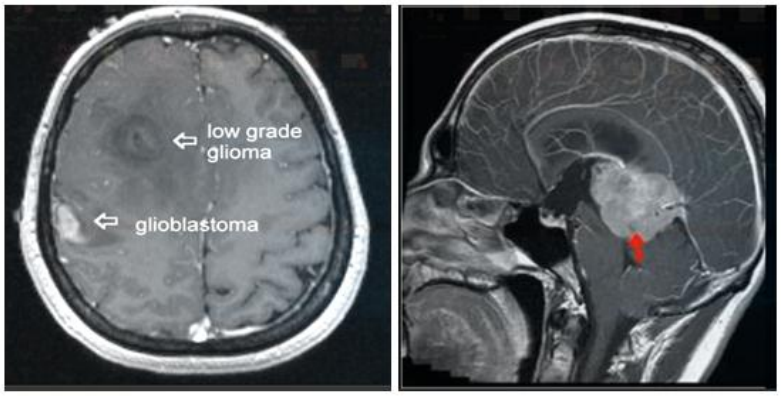

A B

Figure (22) Intracranial tumors that reflect the clinical manifestation for proper diagnosis Figures A,B and C on the top with Figures A,B and C in bottom illustrates these phenomenon (Andreasen, N.C., et al 1988)

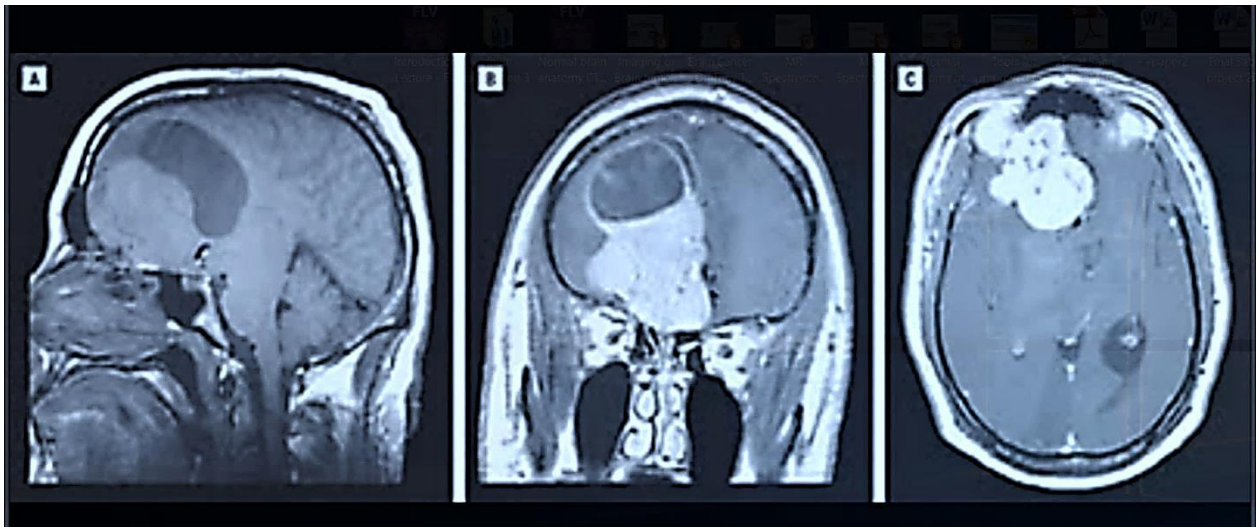

Figure (2-23)

Tumor in Figure (2-23) representing 3D MRI showing the invasion and compression of tumor to normal cells and causing deficit to normal function

(Andreasen, N.C., et al 1988)

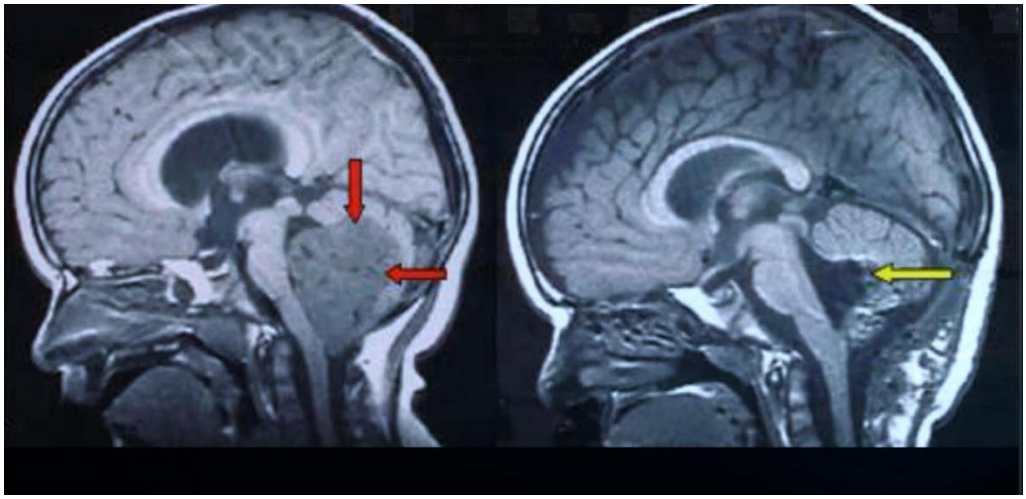

Figure (2-24): Forth ventricle tumor causes obstruction of CSF flows into the subarachnoid space and causes hydrocephalus.

(Andreasen, N.C., et al 1988)

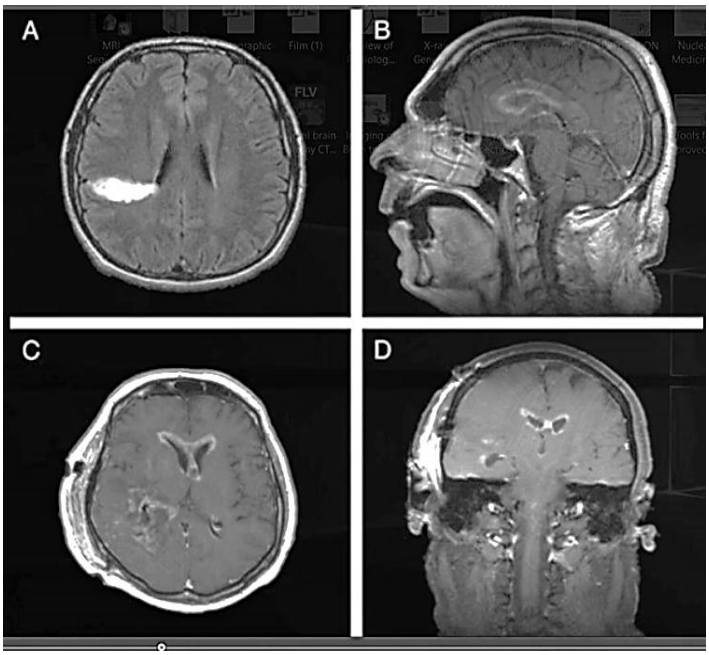

Figure (2-25): Temporal region tumor. Brain swelling due to collection of CSF in subarachnoid space(Andreasen, N.,C et al 1988)

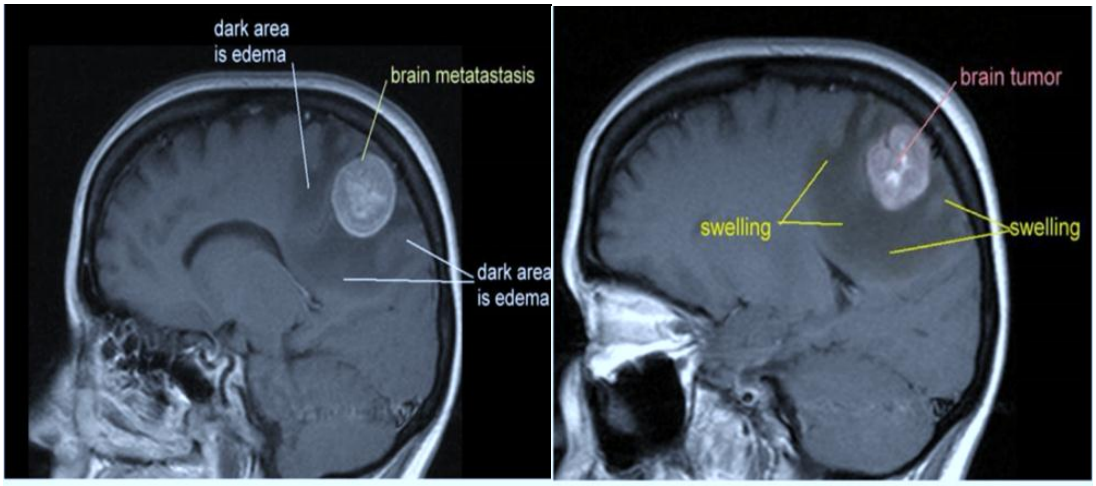

Figure (2-26)

Tumor surrounded by fluid due to the irritation of normal cells and causes edema(Andreasen, N. C., et al 1988)

Tumors often cause swelling or edema which creates pressure on the brain, with headache and nausea. Steroids drugs will decrease the pressure.

2.4.3 Physical Basis of MRS

Strong magnetic fields are necessary for NMR spectroscopy. Even with these high fields, the energy difference between the two spin states is extremely tiny. Irradiation of sample with radiofrequency (RF) energy corresponding exactly to the spine state separation of a specific set of nuclei will cause excitation of those nuclei in the +½ state to the higher -½ state. This electromagnetic radiation falls in the radio and television broadcast spectrum .NMR spectroscopy is therefore the energetically mildest probe used to examine the structure of molecules.

Since all protons have the same magnetic moment, we might expect all hydrogen atoms to give resonance signals at the same field/frequency values. Fortunately for chemistry applications, this is not true. The answer to this question lies with the electron(s) surrounding the proton in covalent compound and ions.

Since electrons are charged particles they move in response to the external magnetic field (Bo so that to generate a second field that opposes the much stronger applied field. This secondary field shields the nucleus from applied field, so the magnetic field must be increased in order to achieve resonance (absorption of RF energy). ***(Nelson, S. M. et al 2002)***

2.4.4 Tetra methyl silane (TMS)

1. Recognition of chemically equivalent hydrogen atoms chemically shifts is measured in relation to the internal reference (TMS).
2. The protons of (TMS) are highly shielded because of strong electron donating capability of silicon.
3. The signal for TMS is well away from most other proton absorptions.

Because protons are shielded by their valence electrons, every proton group experiences a slightly different magnetic field and therefore resonates at different frequencies, measured as the chemical shift away from a reference standard in parts per million (ppm). These differences can be demonstrated by MR spectroscopy (MRS) as spectra whose peaks are attributable to particular metabolites. The appearance of the spectra depends on the settings on the scanner. For example, short TE spectra display peaks attributable to a wide variety of metabolites, including lipids and macromolecules, glutamate and glutamine, and my inositol. ***(Cecil KM and Kos RS,2006***)

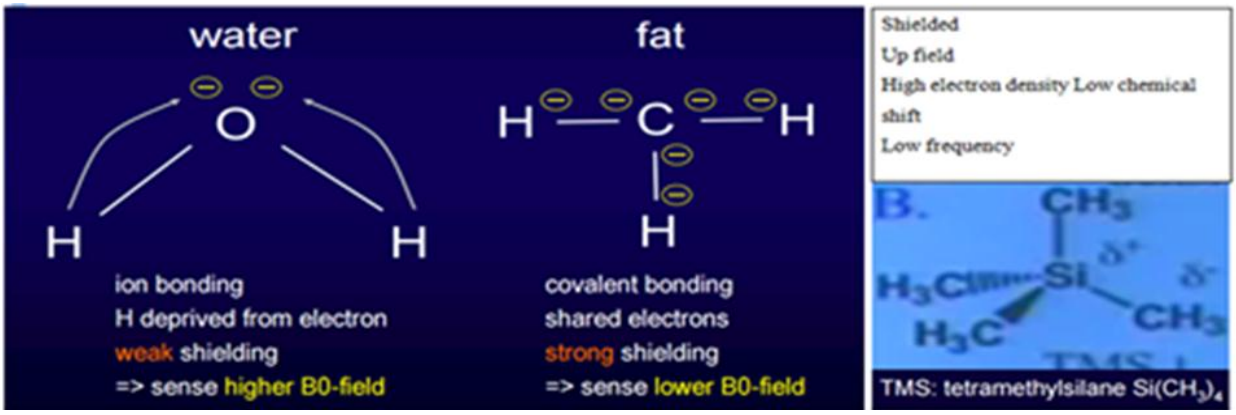

Figure (2-27)

Figure (37) illustrated the protons of (TMS) are highly shielded because of strong electron donating capability of silicon. (Cecil., K.M,et al 2006).

Long echo time (TE) MRS, which is insensitive to lipids and macromolecules, is better at differentiating alanine and lactate .Both long and short TE spectra show N-acetyl aspartate (NAA), choline-containing compounds (Cho), and Creatine/phosphocreatine (Cr). (***Cecil*, *K.M,et al 2006***).

A basic understanding of the physics of MRI is desirable to appreciate how we distinguish and accurately localize tissues in the body. It is also important to help understand the principles of using the ever-increasing number of MRI sequences. Hydrogen atoms or protons are a fundamental building block of all living tissues, principally in the form of water. Protons have an atomic number of 1 with an odd mass number and are MRI – active nuclei. They are used because they are abundant in the body and the best signal is received from them due to their large magnetic moment. ***(Lin DD, C. B et al 2003)***

The proton has a single positive charge and spins on its own axis much like the earth. However, it also precesses like a spinning top. A moving / spinning charge can be considered to be an electrical current and this is in turn induces a magnetic field. So this means that there are billions of spinning protons in the body acting like tiny bar magnets. Under normal conditions, they are all randomly aligned with all their fields cancelling each other out they have no net magnetic moment. When the patient is in the MRI scanner, all the protons align themselves along this external magnetics field, which runs straight down the centre of the tube.

Most of the protons cancel each other out and it is only 1 or 2 unmatched protons per million that give a net magnetic vector aligned longitudinal to the external field, the patient themselves becoming a magnet. Unfortunately, this cannot be measured directly.

The frequency at which protons precess is proportional to the strength of the external magnetic field. A one Tesla external field strength causes the protons to precess at 42.6MHz. This is important in a short burst of energy (in milliseconds) is imparted to the protons in the form of a radiofrequency (RF) pulse. This is done through a coil. The RF pulse is of a specific frequency that can exchange energy with the proton, known as the resonance frequency, which has the same precession frequency as the proton. This can be calculated depending on what tissue is being imaged. Rather than precessing randomly along the external field, the RF causes the protons to precess in step or in phase with each other in the same direction at the same time. This also results in the magnetic vector pointing more sideways – transverse magnetization- and less in the longitudinal direction. When the RF pulse is turned off, the protons start to lost energy while returning to their natural, relaxed alignment within the external magnetic field.

Longitudinal magnetization is regained, which is known as longitudinal or T1 relaxation. Transverse magnetization is lost, which is known as transverse or T2 relaxation. As this occurs they give off a signal that the detector coils pickup.

The rate at which T1 and T2 relaxation occur depends on the tissue in which the protons lie. The resulting differences in signal intensity provide image contrast between tissues in the body. In addition, the density of protons in a tissue will also determine the signal intensity. ***(Lin, D. C. B. ,et al 2003)***

Locating both the volume of tissue and then recognizing the x, y and z coordinating of the signal generated by the protons depends on the use of three gradient coils. These apply a very weak magnetic field (18 – 27millitesla) in addition to the main external field. By imparting energy to specific areas the location of the subsequent signal is established **(*Lin, D. C., et al 2003)***

2.4.2 Single and multiple voxel

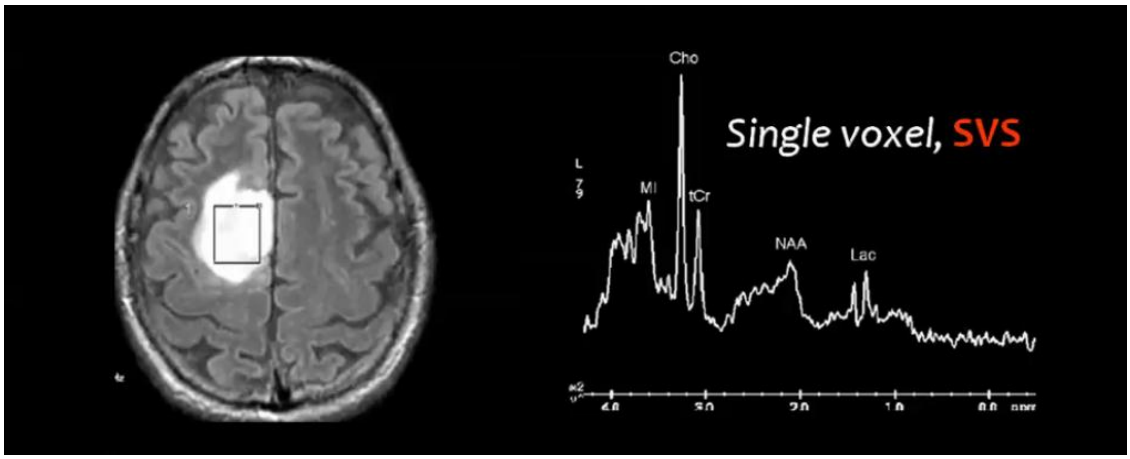

Figure (2-29): Single voxel

Nelson SJ, McKnight TR, Henry RG ,2002

Available on most scanners, result in a high quality spectrum with a short scan time in 3 – 5 minutes, the voxel size 2x2x2($8cm^3$) with good field homogeneity,

usually obtained with short TE since longer TE has decreased signal due to T_2 relaxation.

Single voxel spectroscopy is used to obtain an accurate quantification of the metabolites

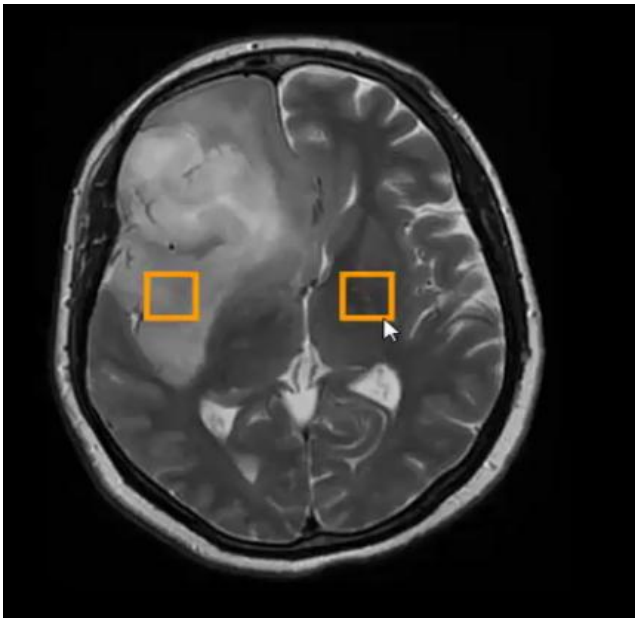

Figure (2-30): Single voxel for comparison

Single voxel is obtaining a spectrum from normal contralateral tissue helps as an internal reference

Nelson SJ, McKnight TR, Henry RG ,2002

Single voxel is obtaining a spectrum from normal contralateral tissue helps as an internal reference. Comparison with the published data may help in selection of techniques and protocols (magnet strength, TR, TE, PRESS or STEAM).

The spectrum of a very small lesion may appear normal because of the partial volume effect of the adjacent normal tissues.

Reduction of the voxel size decreases SNR which is compensate d for gy increase of the number of acquisitions. Use multi – voxel technique with increased the number of encodings to 24(normal 16) to get small voxel with less partial volume

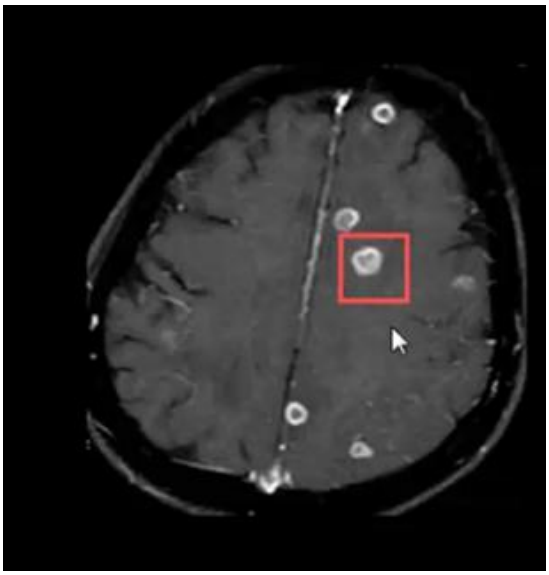

Figure (2-31): Difference between single voxel and multi- voxel
Nelson SJ, McKnight TR, Henry RG, 2002

Table (2) Difference between single voxel and multi- voxel

SVS	**MV SI**
Short TE	Long TE
One voxel	Multi - voxel
Limited region	Many data collected
Fixed gride	Grid may be shifted after acquisition
More accurate	Less accurate
Quantitative measurement	Special distribution

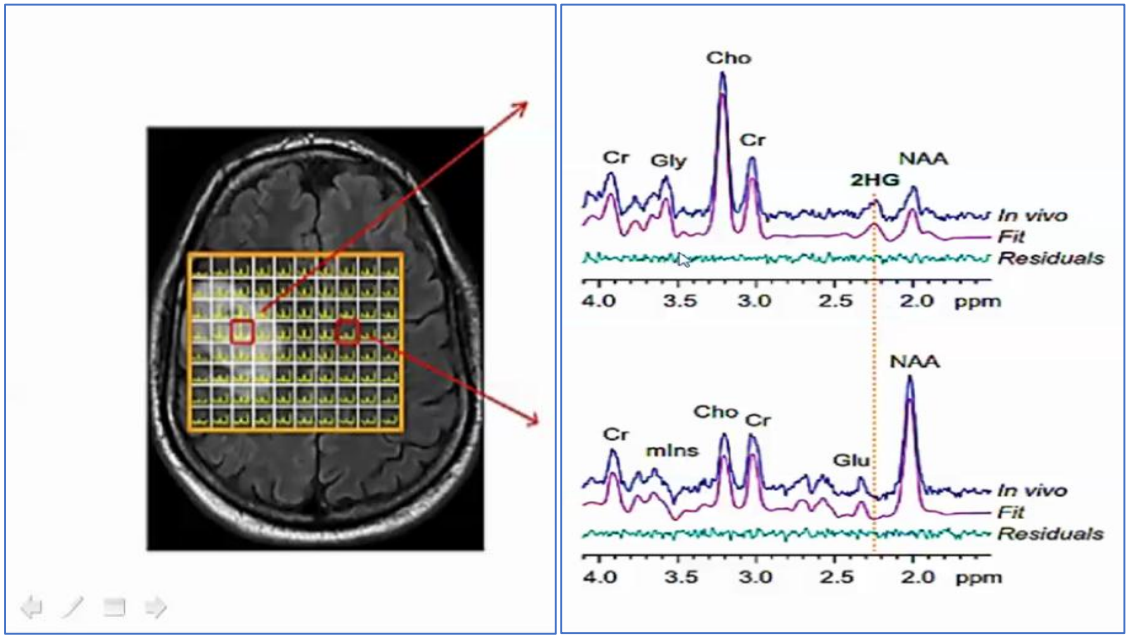

Figure (2-32): Multi-voxel scan

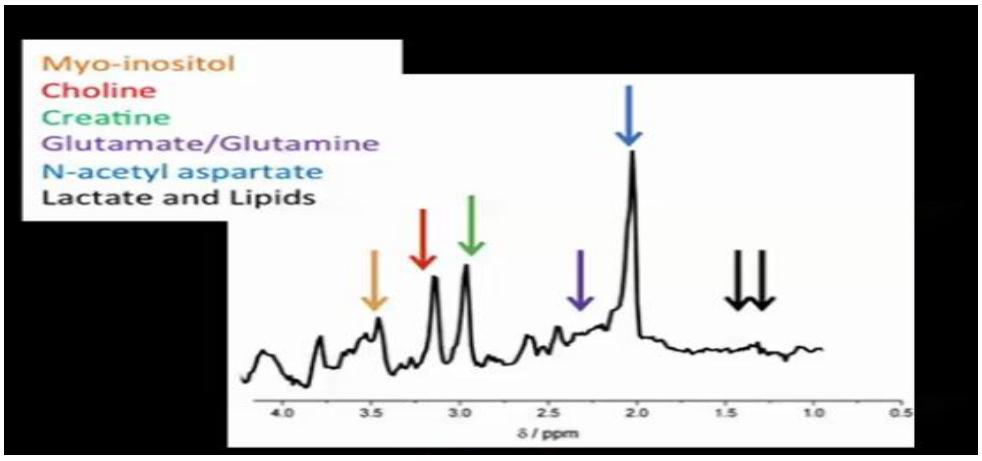

Figure (2-33): MRS Short TE

Nelson SJ, McKnight TR, Henry RG, 2002

Short TE refers to a study in which it varies from 20 to 40ms which has a higher SNR and less signal loss due to T_2 and T_1 weighting than long TE, the short TE

result in a spectrum with more metabolites peaks, these peaks include myoinositol and glutamine.

Peaks overlap is much more common and must be taken during interpretation. MRS spectra obtained with long TE, from 135 – 288 ms, commonly used long TE ranges between 135 – 144 ms. Long TEs have a worse SNR.
More simple spectra due to suppression of some signals which are less noisy but have a limited number of sharp resonances, on long TEs peak of lactate is inverted below the base line, this is important since the peaks of lactate and lipids overlap in this spectrum.

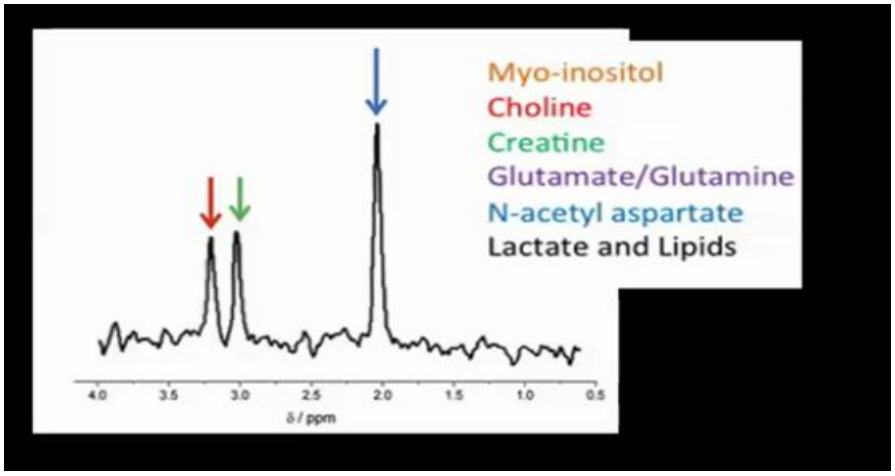

Figure (2-34): MRS long TE

Nelson SJ, McKnight TR, Henry RG (2002)

The peak of lactate when presented projects above the baseline on short TE sequences and inverted below the baseline at long TE sequences and inverts below the base line

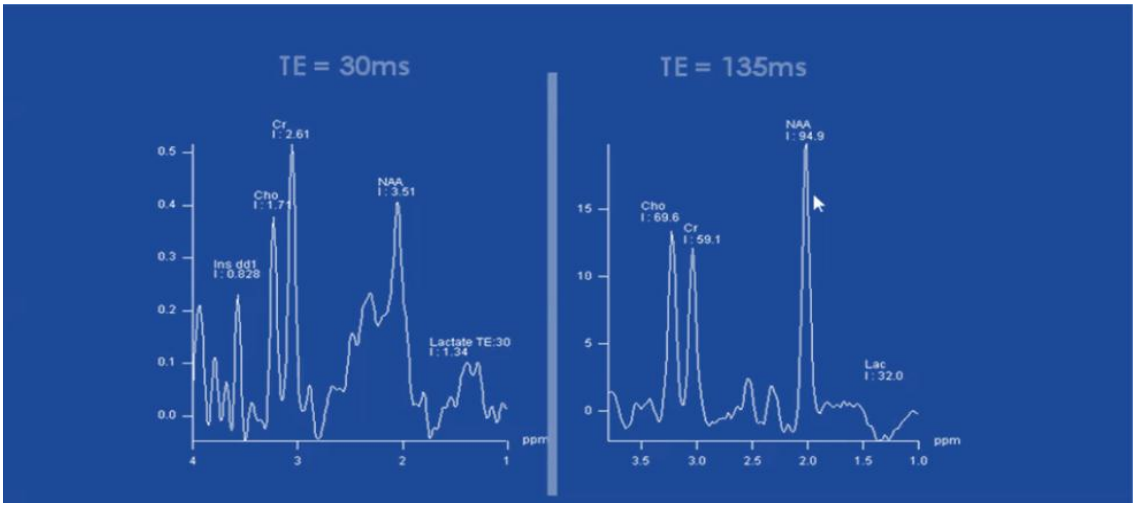

Figure (2-35): comparison short and long TE
Nelson SJ, McKnight TR, Henry RG (2002)

Note the inverted lactate peak (doublet) with long TE acquisition and the more number of sharps resonance with short TE. Cho – Cr – NAA and Myoinositol

3.3.8 Quality of the spectra

An appropriate shimming are used to improve the field homogeneity and an adequate water suppression by a process called CHESS.

Adequate voxel adjustment is used to avoid:

- Bones
- Metals
- Blood vessels
- Blood products
- Air, CSF and fat
- Necrotic areas
- Calcifications

The position of the metabolite signal in the spectrum presents its chemical shift scaled in (ppm), while the area under each peak may represent the metabolite concentration.

A good quality spectrum should presents a flat horizontal baseline with distinct narrow peaks.

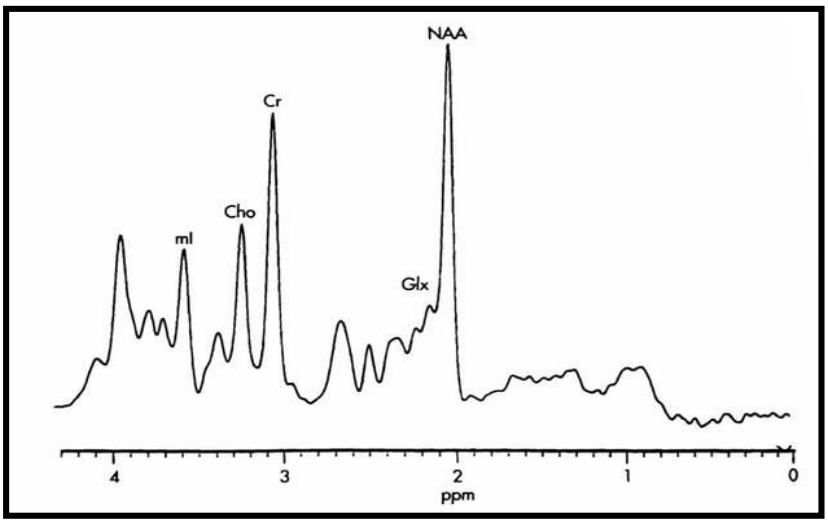

Figure (2-36):

A good quality spectrum should presents a flat horizontal baseline with distinct narrow peaks

(Nelson SJ, McKnight TR, Henry RG 2002)

2. 5 Previous Studies

Elias, R. M., et al (2006) had studied advantage MR imaging technique to diagnosis Intracranial tumors for a significant health problem. The annual incidence of primary and secondary central nervous system neoplasms ranges from 10 to 17 per 100,000 persons. The American Cancer Society and the Primary Brain Tumors in the United States Statistical Report projected that in 2005 in the United States, an estimated 12,760 deaths from intracranial tumors would occur, and that an estimated 43,800 new cases of primary nonmalignant and malignant central nervous system tumors would be diagnosed, respectively. Imaging plays an integral role in intracranial tumor management. Magnetic resonance (MR) imaging in particular has emerged as the imaging modality most frequently used to evaluate intracranial tumors, and it continues to have an ever-expanding, multifaceted role. In general, the role of MR imaging in the workup of Intraxial tumors can be broadly divided into tumor diagnosis and classification, treatment planning, and post treatment surveillance. In addition to conventional MR imaging techniques, a variety of advanced techniques have found their place in clinical practice or are the subject of intense research. These advanced techniques offer more than the anatomic information provided by the conventional MR imaging sequences. They generate physiologic data and information on chemical composition. The current advanced techniques include perfusion imaging, diffusion-weighted imaging (including diffusion-tensor imaging), MR spectroscopy, blood oxygen level–dependent (BOLD) imaging, and the largely experimental molecular imaging. ***(Elias, R., M., 2006)***

Julio, S., et al (2010) had studied how to Obtain a spectrum, that will analyzed, influenced by many factors, namely the physical and chemical characteristics of each metabolite and the compounds in which they are located; the selection of the area to study (cystic, solid, homogeneous, heterogeneous) together with the homogenization of the area (homogenization of the field and the sample, suppression of water signal), choice of the type of technique to be employed (monovoxel or multivoxel) and of the sequence to be used (PRESS, DRESS, SPARS, STEAM) and the choice of the echo time (short or long). Obtaining a spectrum adequate for analysis depends on the correct choice or application of all the above mentioned parameters, plus an appropriate cooperation on the part of the patient; this could give rise to differences observed by different researchers. In material and methods the various parameters used in obtaining the spectrum were mentioned.

However, it is worth pointing out that the spectra obtained at long TE were mainly analyzed due to:- the spectrum obtained is simpler to analyze, quantify and interpret, making the technique more reproducible in daily practice; at long echo times the resulting peak at 1.3 ppm is mainly composed of lactates because lipids have a short echo time and therefore, they would become saturated. ***(Julio, Suarez, et al 2010***)

John, R. H.,et al (2010), had studied MRS that used to determine the degree of malignancy. As a general rule, as malignancy increases, NAA and Creatine decrease, and Choline, lactate, and lipids increase. NAA decreases as tumor growth displaces or destroys neurons. Very malignant tumors have high metabolic activity and deplete the energy stores, resulting in reduced Creatine. Very hyper cellular tumors with rapid growth elevate the Choline levels. Lipids are found in necrotic portions of tumors, and lactate appears when tumors outgrow their blood supply and start utilizing anaerobic glycolysis. To get an accurate assessment of the tumor chemistry, the spectroscopic voxel should be placed over an enhancing region of the tumor, avoiding areas of necrosis, hemorrhage, calcification, or cysts.

Multi-voxel spectroscopy is best to detect infiltration of malignant cells beyond the enhancing margins of tumors. Particularly in the case of cerebral glioma, elevated Choline levels are frequently detected in edematous regions of the brain outside the enhancing mass. Finally; MRS can direct the surgeon to the most metabolically active part of the tumor for biopsy to obtain accurate grading of the malignancy.

MRS cannot always distinguish primary and secondary tumors of the brain from one another. As mentioned above, one key feature of gliomas is elevated Choline beyond the margin of enhancement due to infiltration of tumor into the adjacent brain tissue. Most non-glial tumors have little or no NAA. Elevated alanine at 1.48 ppm is a signature of meningiomas. (***John, R. H., et al 2010***)

Stadlbauer, et al(2006), had studied a technique that detects metabolites, such as n-acetyl aspartate, Choline-containing compounds, Creatine/phosphocreatine, and lactate Measurements of metabolite ratios provide diagnostic information that adds to that obtained by MRI alone. MRS can be valuable in the diagnosis of leukodystrophies and mitochondrial disorders. Providing prognostic information in neonatal hypoxia/ischemia. Differentiating among brain tumors, staging, and identifying a suitable biopsy site Differentiating between tumor progression and radiation necrosis. In most cases, single voxel MRS is used to obtain chemical information from a region of interest measuring 2x2x2 cm; in multivoxel MR spectroscopic imaging (MSRI), the voxel size is 1 cm3. ***(Stadlbauer, et al 2006)***

Law, et al (2003), had studied the process through which the differentiation of high grade gliomas from solitary metastasis. Both lesions show the same HMRS pattern, with high Cho and low NAA. However, the high signal intensity on T2 weighted imaging seen in the perilesional area demonstrates elevated Cho/Cr ratio only in high grade gliomas (Gliomas are the most common and the most studied lesions among neuroepithelial tumors. They originate from glial cells (e.g. astrocytes or oligodentrocytes). Gliomas have an infiltrative nature resulting in neuronal cell damage and decreased NAA. Although conventional MRI with gadolinium-containing contrast media has been useful for characterizing brain tumors, areas of contrast enhancement are not always the most malignant portion of the tumor, because some low-grade tumors show contrast enhancement and a few glioblastomas do not. High- and low-grade tumors cannot therefore be reliably differentiated on the basis of contrast enhancement. ***(Law, et al 2003)***

Grand, et al. (1999*)** had studied how the advanced MRI techniques provide useful, complementary information for grading gliomas, in comparison with conventional MRI. Echo planar diffusion, perfusion MRI and multivoxel proton MRS can offer diagnostic conventional MRI, in the assessment information, not available with of glioma grade. Gliomas, the most frequent primary brain tumors, are histologically heterogeneous, representing a biologic continuum with varying degrees of cellular and nuclear pleomorphism, mitotic activity, vascular proliferation and necrosis. Although conventional MRI with gadolinium-containing contrast media has been useful for characterizing brain tumors. Although single-voxel MRS has been reported to be useful for investigation of gliomas, it is difficult to assess the spatial distribution of spectral changes. Recent developments in MRS have made it possible to obtain chemical-shift imaging (CSI) with high spatial resolution and multiple spectra simultaneously from contiguous voxels. ***(Grand, et al 1999)

Goumnerova, L., et al (2009), had studied A noninvasive technique, that is helpful in understanding the pathophysiology of the different disease processes. It has been used to observe metabolite changes indifferent intracranial abnormalities such as tumors, stroke, tuberculomas, multiple sclerosis, and metabolic brain disorders. Spectroscopic studies on brain tumors have attempted to (a) characterize the different histological types and (b) predict the degree of malignancy of the gliomas. Preoperative grading of gliomas is necessary, because it helps in better treatment planning and management.

Imaging modalities such as computed tomography and MR are unreliable in the grading of different gliomas. Proton nuclear magnetic resonance (‘HNMR) spectroscopy is a noninvasive technique that can provide information on a wide range of metabolites. ***(Goumnerova, L., et al 2009***)

Torni1, C., et al (2013), had studied the necessary to identify the lesion type in patients who have undergone MR for the detection of suspected cerebral tumour. It would be equally important to consider the presence of tumoral tissue infiltrating beyond the enhancement area to be able to differentiate metastases As a final step, it would be necessary to define the malignancy grade by differentiating low grade gliomas (I and II grade) from those at a high grade (III and IV grade). In some cases the morphological study itself, with and without contrast, accomplishes differential diagnoses between low and high grade tumors. Glioblastomas often have typical involvement, conspicuous vasogenic edema, necrotic aspect), different from low grade astrocytic gliomas.

However, in many cases the differential diagnosis is not easy, especially among gliomas of II and III grade with low or no enhancement after contrast .Gliomas characterization is important firstly because it precisely assesses the risk/benefit relationship of the surgical operation. Secondly, it is generally known that, in some cases, the histological examination can underestimate and spectroscopy imaging can be useful to detect the lesion malignancy grade 10-13 correctly, in addition to identifying accurately the biopsy sampling.

Perfusion imaging provides brain vascular maps that identify cerebral tissues on the basis of several hemodynamic parameters.

The parameter that most effectively relates to histological characteristics of cerebral gliomas is CBV that is proportional to the volume of micro vessels supplying an area of interest.
In this case, therefore, the malignancy grade is proportional to the density of the lesion's micro vessels.
Spectroscopy, on the other hand, detects the concentration of some metabolites, always in specific lesion areas. The glioma malignancy grade is directly proportional to the choline peak (which is produced during the synthesis of biological membranes and is, therefore, a marker of replicating cells) and is inversely proportional to the Cho/NAA ratio. ***(Torni1, C. ,et al 2013)***

Harish, P., R.,G., R., K, et al (2012), had studied NAA as a neuronal marker and decreases in all tumors because of the invasiveness of tumor cells within the normal tissue.
Proton MR spectroscopy–visible Cho-containing compounds include acetyl choline, glyceroph membrane turnover and cell proliferation.
Cr/phosphocreatine, an indicator of energy osphocholine, and phosphocholine.
Cho is increased in all tumors because of increased metabolism, shows a variable signal intensity in proton MR spectroscopy of intracranial tumors.
Gliomas have been graded on the basis of NAA/Cho, Cho/Cr, NAA/Cr, and lactate/Cr ratios. NAA/ Cho and Cho/Cr ratios have shown consistency in predicting the tumor grade, we observed NAA peak in only 12 of 37 cases of high-grade gliomas.

The comparison of NAA/ Cho and Cho/Cr ratios in these cases with that of the low-grade gliomas provided a significant difference between the two groups. In the present study, NAA/Cr ratio did not provide any significant correlation with the degree of malignancy.

Most tumor cells have low respiration and high glycolysis rates even when oxygen levels are sufficient for respiration. The high glycolytic rate results in increased accumulation of pyruvate, which converts to lactate, because there is a decrease in the tricarboxylic acid cycle activity in brain tumors.

Alternatively, lactate also may be produced by anaerobic glycolysis in tumors with hypoxia. Increased low-grade gliomas. Lactate in all the low grade gliomas and most high-grade gliomas in the present study suggests that its presence does not correlate with the grade of malignancy. Lipid resonances have been observed in high-grade gliomas on in vivo studies using different echo times, in areas of MR imaging especially.

The presence of NAA in metastases, on in vitro and in vivo studies, is attributed to the presence of normal brain parenchyma in infiltrating lesions or the partial volume effects with adjacent brain tissue.

The presence of a small broad resonance at 2.02 ppm, in five cases, along with resonances at 1.3 ppm and 0.9 ppm is probably attributable to the methylene. (***Harish, P., R.,G., R., K, et al. 2012***)

Kumar, A. K. S. ,et al (2011),

had studied Proton MRS to improve the diagnostic accuracy preoperatively in brain tumors, even obviating stereotactic biopsies in some cases (especially the inoperable tumors), and helping in monitoring the response to therapeutic surgical/medical intervention. The metabolites routinely assessed include Cho, Cr, NAA, Lac and Lipids. Cho from choline-based compounds (acetylcholine, phosphocholine, glycero-phosphocholine), involved in cell membrane bio-synthesis and turnover, is elevated in processes involving increased membrane formation and cell proliferation. Cr from phosphocreatine and creatine is involved in energy metabolism. As Cr resonance intensity is relatively invariant and uniform throughout the normal brain tissue, it is used as an internal standard against which resonance intensities of other metabolites are normalized. However, Cr may be reduced in hyper metabolic and raised in hypo metabolic states. NAA, a neuronal marker, is decreased in processes involving neuronal loss or damage. Lac and lipid peaks are not observed in a normal brain spectrum. Presence of lactate, an end-product of anaerobic glycolysis, is an indirect index of ischemic and hypoxic conditions. A lipid signal may be detected in conditions leading to disruption of cell membranes and myelin sheaths. The typical 1H-MRS characteristics of gliomas include elevated Cho signal with reductions in NAA and Cr peaks; along with lactate/lipid peaks in some cases. Elevation of Cho in mitotic lesions reflects increased membrane synthesis and cellularity.

Elevated Cho/Cr ratio is generally correlated with an increase in tumor malignancy and used as a possible non-invasive index of tumor grading. ***(Kumar, A., K., S.,et al 2011)***

William, G. N., R., et al (1996) represent a cooperative group of 15 institutions that examined the feasibility of using metabolic features observed in vivo with ‘H-magnetic resonance (MR) spectroscopy to characterize brain tumors of the glial type. The institutions provided blinded, centralized MR spectroscopy data processing along with independent central review of MR spectroscopy voxel placement, composition and contamination by brain, histopathological typing using current World Health Organization criteria, and clinical data, Proton 'H-MR spectroscopy was performed using a spin-echo technique to obtain spectra from 8-cc voxels in the tumor and when feasible in the contralateral brain. Eighty-six cases were assessable, 41 of which had contralateral brain spectra. Glial tumors had significantly elevated intensities of choline signals, decreased intensities of creatine signals, and decreased intensities of N- acetyl asp art ate compared to brain. Choline signal intensities were highest in astrocytomas and anaplastic astrocytomas, and creatine signal intensities were lowest in glioblastomas. However, whether expressed relative to brain or as intratumoral ratios, these metabolic characteristics exhibited large variations within each subtype of glial tumor. The resulting overlaps precluded diagnostic accuracy in the distinction of low- and high-grade tumors. Although the extent of contamination of the

H- MR spectroscopy voxel by brain had a marked effect on metabolite concentrations and ratios, selection of cases with minimal contamination did not reduce these overlaps.

Thus, each type and grade of tumor is a metabolically heterogeneous group. Lactate occurred infrequently and in all grades. Mobile lipids, on the other hand, occurred in 41% of high-grade tumors with higher mean amounts found in glioblastomas. This result, coupled with the recent demonstration that intratumoral mobile lipids correlate with microscopic tumor cell necrosis, leads to the hypothesis that mobile lipids observed in vivo in EH-MR spectroscopy may correlate independently with prognosis of individual patients.

(William, G. N., R.,et al 1996)

Ellen, A., B., R.,et al (2001) in this study, investigate a panel of normal human prostate cells (HPCs) and tumor cells derived from metastases were studied by 1H NMR spectroscopy to determine whether the malignant transformation of HPCs results in the elevation of choline compounds. Although an elevated choline signal has been observed previously in clinical studies, the contribution of the different Cho compounds to this elevation, as well as their quantification, has not been established until now. Here we have shown that HPCs derived from metastases exhibit significantly higher phosphocholine as well as glycerophosphocholine levels compared with normal prostate epithelial and stromal cells.

Thus the elevation of the choline peak observed clinically in prostate cancer is attributable to an alteration of phospholipid metabolism and not simply to increased cell density, doubling time, or other nonspecific effects. Androgen deprivation of the androgen receptor positive cell lines resulted in a significant increase of choline compounds after chronic androgen deprivation of the LNCaP cell line and in a decrease of choline compounds after a more acute androgen deprivation of the LAPC-4 cell line.

These data strongly support the use of proton magnetic resonance spectroscopic imaging to detect the presence of prostate cancer for diagnosis, to detect response subsequent to androgen ablation therapy, and to detect recurrence. (***Ellen, A., B., R.,et al 2001)***

Caroline, R. M., R.,et al (1998), found that biochemical differences between dyslexic men and controls in the left temporo-parietal lobe (ratio of choline-containing compounds [Cho] to N-acetyl aspartate [NA] $p \geq 0{\cdot}01$) and right cerebellum (Cho/NA, $p \geq 0{\cdot}01$; creatine [Cre] to NA 0·05; (not significant). We found lateral biochemical differences in dyslexic men in both these brain regions (Cho/NA in temporo-parietal lobe, left vs. right, $p \geq 0{\cdot}01$; Cre/NA in cerebellum, left vs. right, $p \geq 0{\cdot}001$). They found no such lateral differences in controls. There was no significant relation between the degree of contralateral chemical difference and handedness in dyslexic or control men. Interpretation We suggest that the observed differences reflect changes in cell density in the temporo-parietal lobe in developmental dyslexia

and that the altered cerebral structural symmetry in dyslexia is associated with abnormal development of cells or intracellular connections or both. The cerebellum is biochemically asymmetric in dyslexic men, indicating altered development of this organ. These differences provide direct evidence of the involvement of the cerebellum in dyslexic dysfunction. ***(Caroline, R. M., R.,et al 1998)***

Alessandro, B. M. H. C. ,et al (2003) ,study shows that patients with bipolar disorder have a regional reduction of NAA relative signals, suggesting neuronal damage or malfunction of the hippocampus.

As suggested by other studies, neuronal pathology in the hippocampus may be involved in the pathophysiology of bipolar disorder and in susceptibility to psychosis. Bio- Psychiatry 2003;53:906–913 © 2003 Society of Biological Psychiatry The results of this study indicate selective reductions of NAA measures in HIPPO of patients with bipolar disorder. None of the other regions sampled with 1H-MRSI or the volume of the hippocampal area showed differences between patients and control subjects. It is difficult to attribute these NAA reductions to hippocampal volume changes because we did not find any correlation between metabolite ratios in HIPPO and its volume. It is also problematic to attribute hippocampal NAA differences to mood changes because the data in the patients studied both while depressed and while manic or hypomanic did not suggest any difference in HIPPO or other brain regions.

As in our previous studies in schizophrenia, we did not find any correlation in patients with bipolar disorder between HIPPO NAA measures and clinical measures or clinical ratings. Because NAA measures reflect neuronal integrity, the results of our study suggest neuronal pathology specifically in HIPPO of patients with bipolar disorder. Some limitations of this study should be acknowledged.

The large majority of patients studied were being treated with various antipsychotics and mood stabilizers; therefore, we cannot definitively exclude a pharmacologic effect on our results. Comparison of the seven drug-free patients with control subjects revealed a significant reduction of NAA/CRE in HIPPO, however .Further statistical analyses within the patients group did not reveal any significant effect of drug treatment. Moreover, recent studies have shown that treatment with antipsychotics tends to increase NAA levels in dorsolateral prefrontal cortex. (***Alessandro, B. M. H. C. ,et al (2003***)

Chapter three

Materials and methods

Chapter three

Materials and Methods

3.1 Materials

The study was conducted during the period extended from 2014 up to 2017, using 1.5 Tesla superconducting Syngo MRI system with 25mT/m maximum gradient potential at Neuro-Surgery and Oncology department at Jazan- Saudi Arabia. One hundred twenty eight (128) participants were selected for the purpose of investigation. 89(69.5%) were males individuals and 39(30.5%) were females individuals were selected who were suffering from different types of gliomas. The participants mean age was 47.08 ±18.1 ranged from 3-86years. No participant had undergone radiotherapy or chemotherapy.

The first criterion for acceptance of MR spectroscopy data from an individual case included absence of any artifacts resulting from miscalibration or misadjustment of shimming, eddy- current correction, or water suppression, which interfere with analysis of metabolite intensities. The second criterion was an adequate signal-to-noise ratio to permit reproducible peak area integration. The third criterion, applicable to NMR spectra from voxels placed near the skull, was absence of contaminating lipid signals, which overlap or distort other peaks in the spectrum.

3.1.2 inclusion criteria

Patients with newly diagnosed or recurrent primary brain tumors of the glial subtype were examined. The initial criteria for inclusion in this study were:

- Acceptable quality of the spectrum
- Evidence on MR imaging of a tumor occupying at least half the volume of the 8-cc MR spectroscopy voxel
- Accepted recurrent cases if they had adequate objective clinical evidence of recurrence of tumor including rebiopsy and/or diagnostic MR imaging scans.

3.1.3 Excluded criteria

The study exclude all the patients who subjected to chemotherapy or radiotherapy

4.2.1 Methods

The patient lies supine on the examination couch with their head within the head coil, the head is adjusted so that the interpupillary line is parallel to the couch and the head is straight, the longitudinal alignment light lies in the midline, and the horizontal alignment light passes through the nasion and straps and foam pads are used for immobilization.

Axial (Axial/oblique SE/FSE PD/T2). Plot on central sagittal the Slices may be angled so that they are parallel to the anterior–posterior commissure axis of lateral ventricles, enough scans for brain from vertex to foramen Magnum. Scout MR images were obtained in two or three planes through the brain to define the region of placement of (2×2×2) 8-cc MR spectroscopy voxels. Voxels were placed to maximize their content of viable tumor.

After a sagittal localizer to get an accurate assessment of the tumor chemistry, the spectroscopic voxel was placed over an enhancing region of the tumor, avoiding areas of necrosis, hemorrhage, calcification, and cysts are necessary to limit brain contamination. Each patient was examined by both short TE (2000/35) (TR/TE) and long TE (1500/144) sequences.

Perfusion and spectroscopy imaging quantitative data were analyzed blindly by experienced neuroradiologist using a dedicated post-processing workstation. Perfusion CBV maps were evaluated by detecting the normalized maximum value of the lesion in relation to the contra lateral normal white matter value (rCBV). With reference to spectroscopy, the maximum Cho/NAA ratio of a voxel selected in the solid tumor area was calculated. In addition, the presence of lactate peak was also taken into account.

Technical quality-control procedures performed on phantoms to include calibration of transmitter adjustment, global shimming to adjust for static Bo inhomogeneity, eddy current adjustments, local shimming to adjust for local static and dynamic Bo inhomogeneity, and calibration of water suppression.

using fast low-angle shot (FLASH). Wherever feasible, 'H-NMR spectra were obtained both from the tumor and the mirror-image region in the contralateral brain. Global and localized shimming on the water proton was performed to obtain less than 25 Hz and 10 Hz full width at half-maximum, respectively, from brain. Spectra were localized using the spin-echo method along with chemical shift selective water suppression.

A single-voxel method, rather than multivoxel chemical shift imaging, was selected because of the feasibility of implementation in clinical imagers.

The spin-echo method was selected based partly because of its signal-to- noise advantage over the stimulated echo method.

4.2.2 MRI brain protocol for K.F.C hospital south region (Gazan)

3.2.2.1. Scout images (localizer)

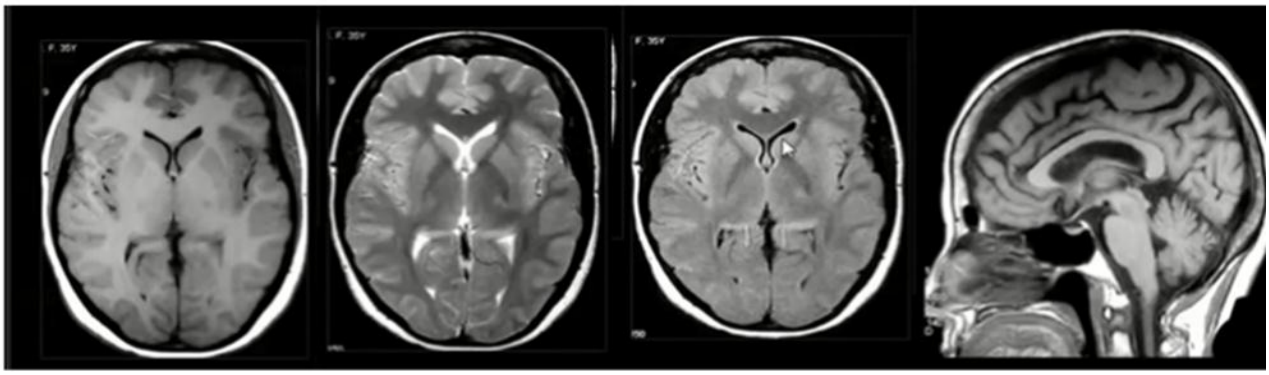

Axial T1 ***Axial T2*** ***Axial FLAIR*** ***Sagittal***

Figure (3-28) the imaging sequence

1. Figure (3-28) Shows the images of the starting point for conventional MRI
2. Choice the appropriate image plane for the imaging cross sections (localizer) for planning .
3. Sections are acquired
4. Radiologist ordered to give the patient contrast media according to their query
5. Gadolinium – DTP was used in most cases
6. Dose depends on the age and weight of the patient as a general rule

7. Contrast injected by automatic injector to control the volume , rate and time of injection
8. Tumors either enhanced by contrast media (CM) or no enhancement
    - No enhancement
    - Enhancement
9. Enhancement patterns
    - Homogenous
    - Heterogeneous
    - Ring (Marginal)
    - Serpigenous
10. Mass effect
    - Effacement of the cortical sulci
    - Compression of the ventricle
    - Shift of the midline structures
11. MRS ordered to catograte the tumor according to metabolite curve

In the single voxel spectroscopy (SVS) the signal is obtained from a voxel previously selected. This voxel is acquired from a combination of slice-selective excitations in three dimensions in space, achieved when a RF pulse is applied while a field gradient is switched on. It results in three orthogonal planes and their intersection corresponds to VOI**.**

3.2.2.2 Reporting a brain tumor

For systemic report to be accepted the following criteria were included

Tumor / Mass	**Description**
Definition	Well defined/ ill defined
Shape	Oval shape
Site	Fronto-parietal
size	4×3 cm
Enhancement	Homogenous/ heterogeneous
Edema	Grading according to a mount of edema
Mass effect	Effacement of Sulci, deviation of ventricles
Normal finding	Posterior. Fossa, sinuses

3.2.2.3 MRS Techniques

The H-MRS acquisition usually starts with anatomical images, which are used to select a volume of interest (VOI), where the spectrum will be acquired. For the spectrum acquisition, different techniques may be used including single- and multi-voxel imaging using both long and short echo times (TE). Each technique has advantages and disadvantages and choosing the right one for a specific purpose is important to improve the quality of the results.

3.2.2.4 Single-Voxel Spectroscopy

In the single voxel spectroscopy (SVS) the signal is obtained from a voxel previously selected. This voxel is acquired from a combination of slice-selective excitations in three dimensions in space, achieved when a RF pulse is applied while a field gradient is switched on. It results in three orthogonal planes and their intersection corresponds to VOI. Therefore much effort has been forth in the research and development of molecular imaging techniques to detect abnormal behavior of tissues.

Gradient echo

These sequences were developed to reduce scan times. This is achieved by giving a shorter RF pulse leading to less disruption to the magnetic vectors. It has particular application in identifying calcific deposits and blood degradation products.

STIR (Short Tau Inversion Recovery) imaging

This sequence is heavily T2 weighted, so that fluid and edema return high signal intensity. In addition, it is designed to cancel out the signal from fat. This provides images in which areas of pathology are clearly visible as bright areas within a dark low signal background. The sequence is of particular use in musculoskeletal imaging as it nullifies the signal from normal bone marrow.

Diffusion Weighted Imaging (DWI)

Diffusion Weighted MRI provides image contrast that is dependent on the molecular motion of water, which may be altered by disease. It reduces the MR signal due to the diffusion of water molecules along a field gradient.

The use of bipolar strong gradient pulses and suitable pulse sequences allows the acquisition of diffusion weighted images

Diffusion weighted imaging was used as an important method in the assessment of brain cases diagnosis by the Creatine reduction, and choline, lactate, and lipids elevation. To get an accurate assessment of the tumor chemistry, the spectroscopic voxel should be placed over an enhancing region of the tumor, avoiding areas of necrosis, hemorrhage, calcification, or cysts as the same method mentioned by Clark. (***Clark, et al1998)***

Multi-voxel spectroscopy was used to detect infiltration of malignant cells beyond the enhancing margins of tumors. Particularly in the case of cerebral glioma, elevated choline levels are frequently detected in edematous regions of the brain outside the enhancing mass.

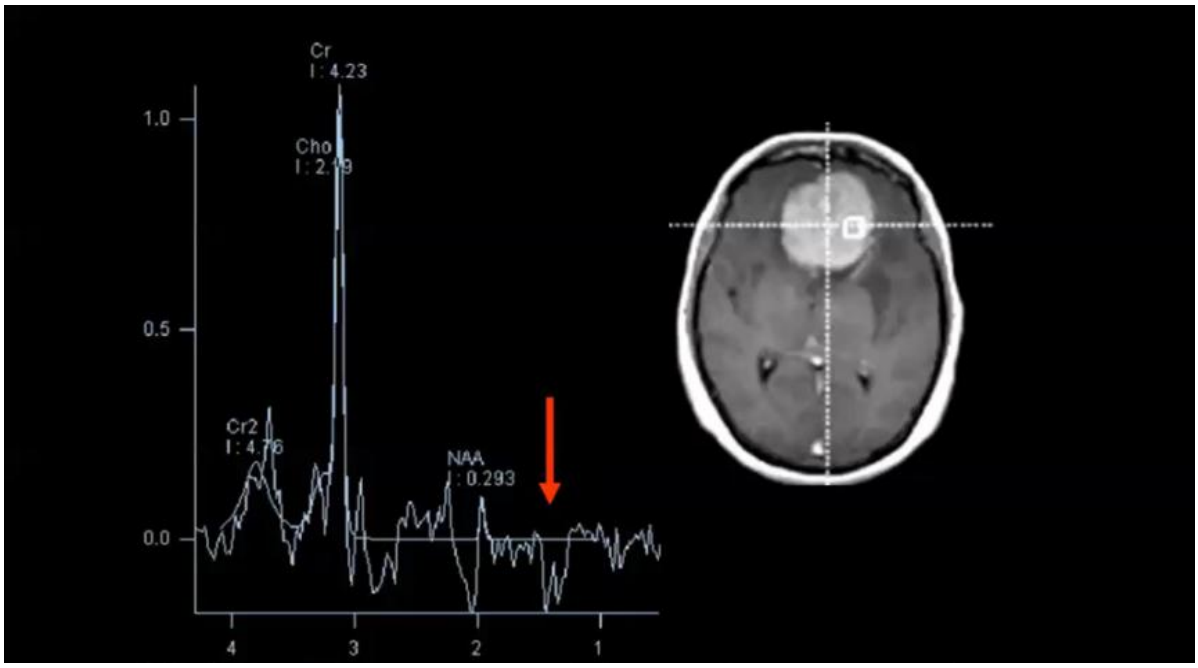

Figure (3-37)

MRS image with long TE 135msec showed absence of NAA peak ,elevation of choline(cho) and double inverted peak at 1.48 ppm that points to lactate.

Lipids (Lip)

K.F. Central hospital South region – Gazan

There are two peaks of lipids at 1.3ppm and 0.9 ppm, there are components of cell membranes not visualized on long TE they have very short relaxation time. These peaks are absent in the normal brain and presence of lipid may result from improper voxel selection, lipid peak is seen in necrotic metastases and primary malignant tumors.

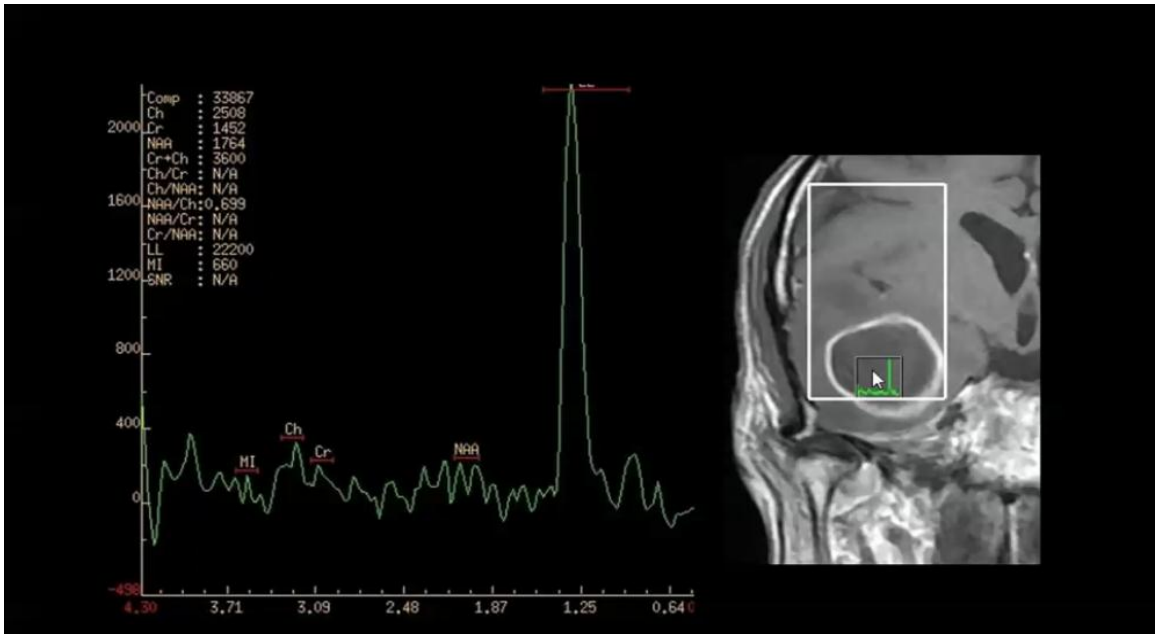

Figure (3-38): MR spectroscopy of the right temporal lesion showing significant elevation of the Lipid / Lactate peaks

K.F. Central hospital South region – Gazan

MR spectroscopy of the right temporal lesion showing significant elevation of the Lipid / Lactate peaks; predominantly within the central portion of the lesion as well as within the enhancing rim with evident depression of the neural markers; N-acetyle aspartate(NAA) and Creatine(Cr)as well as Choline(Cho).

Astrocytomas are classified into low grade benign and high grade malignant tumors, high grade gliomas include anaplastic gliomas and glioblastoma multiforme, and high grade gliomas have higher Cho and lower NAA than low grade ones.

Higher Cho / Cr, Cho/NAA are reported in high grade than in low grade gliomas, Cho / Cr is the most frequency used ratio, threshold value of 2.0 for Cho /Cr is used to differentiate low from high grade gliomas.

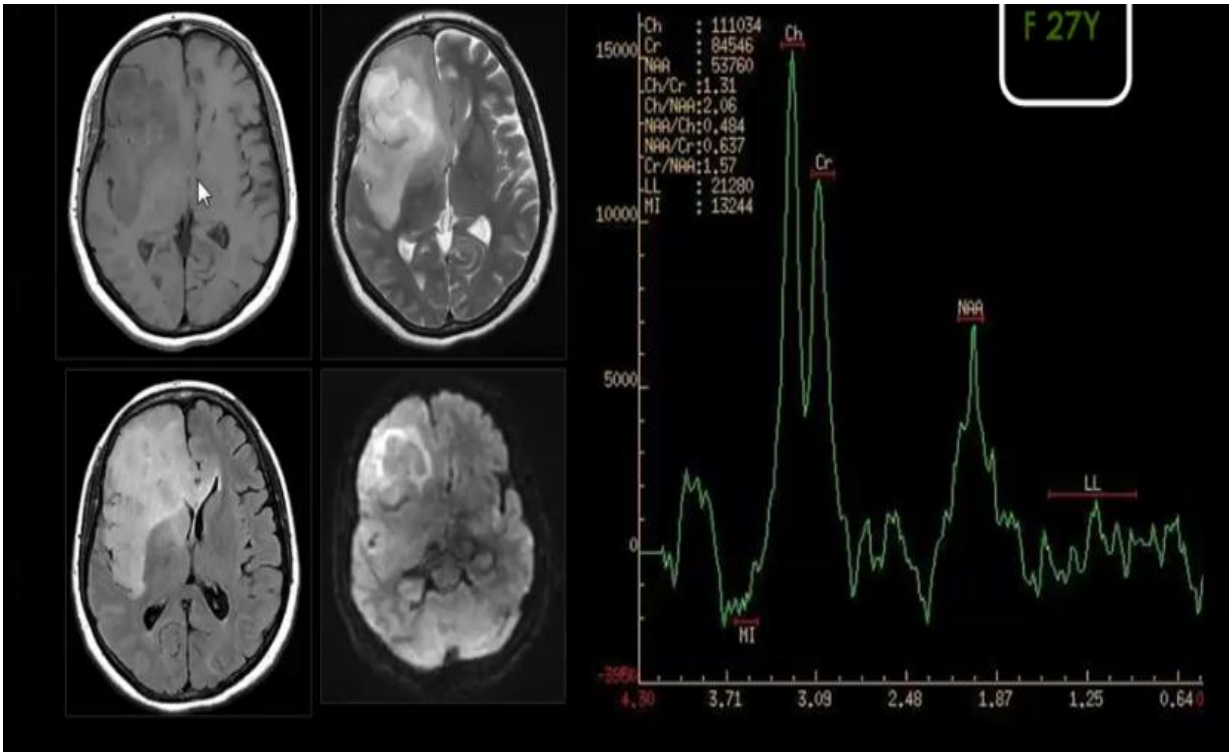

Figure (3-39)

Gliomatosis cerebri with elevated choline and reduced lipid

K.F. **Central hospital South region – Gazan**

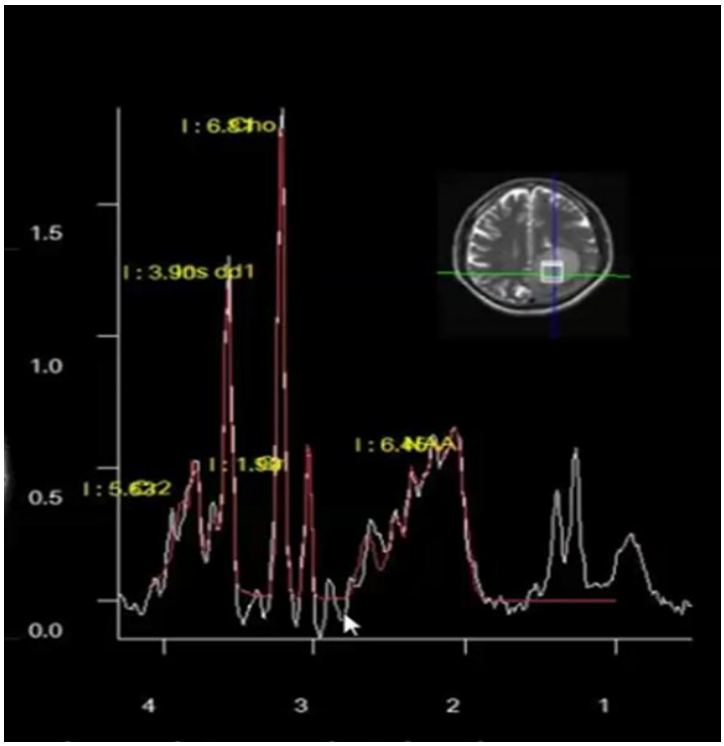

Figure (3-40)

Primary CNS lymphoma with elevated choline reduced NAA

K.F.C hospital South region – Gazan

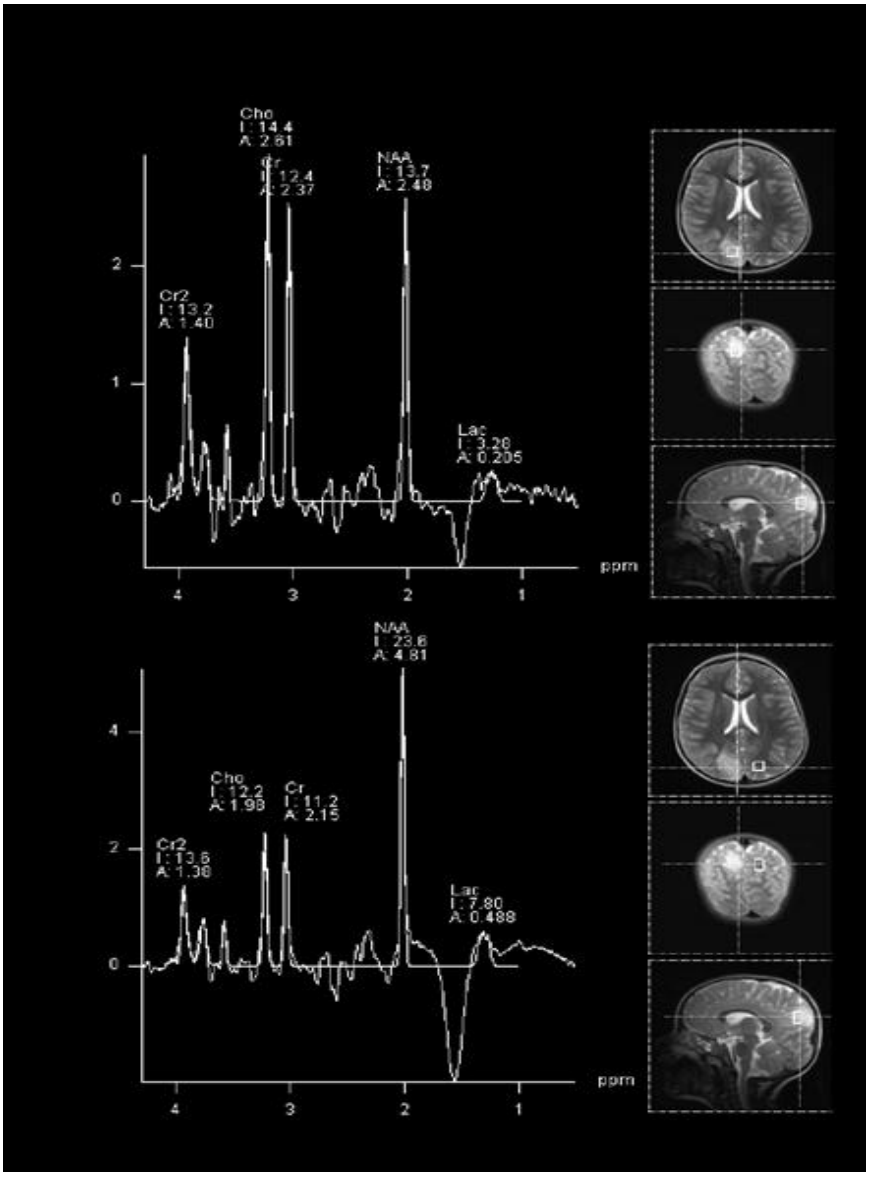

Figure (3-41)

MRS with elevated Cho/NAA in lesion 14.4/13.7= 1.1 relative to contralateral normal brain 12.2/23= 0.5

K.F. Central hospital South region – Gazan

Chapter four

Results

Chapter four

4.1 Results

Result of Diagnostic value of MRI and MRS in characterization of brain tumors

Table No (1) Distribution of study sample according age, frequency and percentages

Age	Frequency	Percentages (%)
<10	5	3.9
11-20	9	7.0
21-30	10	7.8
31-40	16	12.5
41-50	34	26.6
51-60	30	23.4
61+	24	18.8
Total	128	100.0(%)

Table No (2) detailed distribution of tumor territory in the brain site across tabulated with age

		Age						Total
		11-20	21-30	31-40	41-50	51-60	>60	
Right Parietal	Count	1	0	0	3	8	2	14
	% of Total	.8%	.0%	.0%	2.3%	6.3%	1.6%	10.9%
Left Temporal	Count	2	0	0	4	4	3	13
	% of Total	1.6%	.0%	.0%	3.1%	3.1%	2.3%	10.2%
Right Temporal	Count	0	0	1	2	0	2	5
	% of Total	.0%	.0%	.8%	1.6%	.0%	1.6%	3.9%
Extra-axial	Count	0	0	3	0	1	3	7
	% of Total	.0%	.0%	2.3%	.0%	.8%	2.3%	5.5%
Left Parietal	Count	0	0	4	2	0	3	9
	% of Total	.0%	.0%	3.1%	1.6%	.0%	2.3%	7.0%
Left Frontal	Count	1	0	5	1	3	3	13
	% of Total	.8%	.0%	3.9%	.8%	2.3%	2.3%	10.2%
Right Frontal	Count	0	2	0	6	1	2	11
	% of Total	.0%	1.6%	.0%	4.7%	.8%	1.6%	8.6%
Occipital	Count	0	1	1	5	6	1	14
	% of Total	.0%	.8%	.8%	3.9%	4.7%	.8%	10.9%
Intra- axial	Count	0	2	1	0	3	0	6
	% of Total	.0%	1.6%	.8%	.0%	2.3%	.0%	4.7%
Thalamus	Count	0	0	0	0	2	0	2
	% of Total	.0%	.0%	.0%	.0%	1.6%	.0%	1.6%
Left middle and Interior cranial fossa	Count	0	1	0	0	1	0	2
	% of Total	.0%	.8%	.0%	.0%	.8%	.0%	1.6%
Left parasagittal	Count	0	0	0	1	0	0	1
	% of Total	.0%	.0%	.0%	.8%	.0%	.0%	.8%
Posterior fossa	Count	0	1	0	0	0	1	2

	% of Total	.0%	.8%	.0%	.0%	.0%	.8%	1.6%
Trigone of right lateral ventricle	Count	1	0	0	0	0	0	1
	% of Total	.8%	.0%	.0%	.0%	.0%	.0%	.8%
Level of Sylvain aqueduct	Count	0	0	0	0	0	1	1
	% of Total	.0%	.0%	.0%	.0%	.0%	.8%	.8%
Superior vermis of left cerebi	Count	1	0	0	0	1	0	2
	% of Total	.8%	.0%	.0%	.0%	.8%	.0%	1.6%
Left cerebellopontine angle and petrus apex	Count	0	0	1	2	1	0	4
	% of Total	.0%	.0%	.8%	1.6%	.8%	.0%	3.2%
Left orbital apex	Count	0	0	0	0	0	1	1
	% of Total	.0%	.0%	.0%	.0%	.0%	.8%	.8%
Right cerebellar hemisphere	Count	1	0	0	0	0	0	1
	% of Total	.8%	.0%	.0%	.0%	.0%	.0%	.8%
Hypothalamus	Count	1	0	0	0	0	0	1
	% of Total	.8%	.0%	.0%	.0%	.0%	.0%	.8%
Under flax	Count	0	0	0	1	0	0	1
	% of Total	.0%	.0%	.0%	.8%	.0%	.0%	.8%
Bi-frontal lobes	Count	0	1	0	2	0	2	5
	% of Total	.0%	.8%	.0%	1.6%	.0%	1.6%	4.0%
Corpus Callosum	Count	1	0	1	0	0	0	2
	% of Total	.8%	.0%	.8%	.0%	.0%	.0%	1.6%
Basal ganglia	Count	0	1	2	1	1	0	5
	% of Total	.0%	.8%	1.6%	0.8%	.8%	.0%	3.9%
Fronto-temporal and Insular cortex	Count	0	0	1	0	2	0	3
	% of Total	.0%	.0%	.8%	.0%	1.6%	.0%	2.4%
Anterior horn of lateral ventricle	Count	0	0	0	1	0	1	2
	% of Total	.0%	.0%	.0%	.8%	.0%	.8%	1.6%
Total	Count	9	9	20	31	34	25	128
	% of Total	7.0%	7.0%	15.6%	24.2%	26.6%	19.5%	100.0%
	P-value= 0.006							

Table No (3) distribution of study sample according to Radiologist diagnosis for the brain lesions

Diagnosis	*Frequency*	*Percentages (%)*
Astrocytoma*	58	45.3
Gliomatosis Cerebri/ Glioblastic Multiform/ (GBM)/ Oligodendroglioma	44	34.4
Meningioma	8	6.3
Metastatic	3	2.3
Lymphoma	2	1.6
Ependymal tumors **	13	10.1
Total	128	100.0 (%)

**The Classification of astrocytoma is divided basically into Astrocytoma, WHO grade I (AI), Astrocytoma, WHO grade II (AII),Anaplastic astrocytoma, WHO grade III (AA III), Glioblastoma multiforme, WHO grade IV (GBM IV) ,pilocytic astrocytoma and Giant cell astrocytoma.*

** Ependymal tumors (including Ependymoma *and Subependymoma)*, 5 cases were Ependymoma and 8 were Subependymoma

Table No (4) Perfusion-MRI (rCBV) for lesions characteristics

Perfusion Character	*Frequency*	*Percentages (%)*
Normal	56	43.8
Hypo- perfused	38	29.7
Hyper- perfused	34	26.6
Total	128	100.0 (%)

***Table No (5) Cross tabulation between the MRS Metabolite values and Perfusion-MRI (rCBV),* STEAM and PRESS Techniques*Long TE (1500/144) and Short TE (2000/35)**

	NAA	Cho	Cr	Cho/ NAA	Cho/ Cr	NAA/ Cr	Lactate	Lip
Perfusion-MRI (rCBV) P-Value	.944 ±.8 (.032)	1.25 ±1.1 (.309)	1.30 ±1.2 (.800)	1.83 ±1.2 (.000)	2.45 ±.96 (.000)	1.28 ±.68 (.677)	1.33 ±.33 (.225)	.97 ±.33 (.865)
STEAM P-Value	.94 ±.89 (.380)	1.25 ±1.1 (.659)	1.30 ±1.2 (.139)	1.83 ±1.2 (.403)	2.45 ±.9 (.291)	1.28 ±.6 (.770)	1.33 ±.3 (.994)	.97 ±.3 (.822)
PRESS P-Value	.94 ±.89 (.380)	1.25 ±1.1 (.659)	1.30 ±1.2 (.139)	1.83 ±1.2 (.403)	2.45 ±.96 (.291)	1.28 ±.68 (.770)	1.33 ±.33 (.994)	.97 ±.33 (.822)

Table No (6) Cross tabulation between the MRS Metabolite values and the diagnosis of brain tumors*Long TE (1500/144) and Short TE (2000/35)

Diagnosis	NAA	Cho	Cr	Cho/ NAA	Cho/ Cr	NAA/ Cr	Lactate	Lip
Astrocytoma	1.05 ±1.04	1.41 ±1.44	1.35 ±1.34	1.67 ±1.01	2.23 ±.87	1.23 ±.61	1.40 ±.41	.865 ±.12
GliomatosisCerebri/ GlioblasticMultiform/ (GBM)/and Oligodendroglioma	0.71 ±.43	1.04 ±.74	1.22 ±.91	2.21 ±1.57	2.87 ±1.01	1.35 ±.867	1.28 ±.30	1.08 ±.46
Meningioma	0.76 ±.27	0.72 ±.31	0.91 ±.44	1.26 ±.349	2.07 ±.950	1.14 ±.203	1.33 ±.00	.900 ±.00
Metastatic	0.97 ±.56	1.22 ±.104	1.41 ±1.703	2.04 ±.505	2.88 ±.085	1.55 ±.593	-	-
Lymphoma	2.73 ±2.92	2.22 ±2.19	3.41 ±3.79	1.08 ±.25	1.39 ±.30	1.19 ±.00	-	-
Ependymoma	0.83 ±0	1.15 ±.00	0.41 ±.00	1.38 ±.00	2.80 ±.00	2.02 ±.00	-	-
P-value	0.029	0.369	.187	0.141	0.004	0.818	0.736	0.624

***Table No (7) Cross tabulation between the radiologist diagnosis of brain tumors* and the lesion Perfusion-MRI (rCBV) results**

Diagnosis * Perfusion-MRI (rCBV) Cross tabulation					
Diagnosis /*P-value=0.001*		Perfusion-MRI (rCBV)			Total
		Hyper-perfusion	Normal	Hypo-perfusion	
Astrocytoma	Count	12	20	26	58
	% of Total	9.4%	15.6%	20.3%	54.7%
GliomatosisCerebri/	Count	21	18	5	44
GlioblasticMultiform/ (GBM)/and Oligodendroglioma	% of Total	16.4%	14.1%	3.9%	34.4%
Meningioma	Count	1	2	5	8
	% of Total	0.8%	1.6%	3.9%	6.2%
Metastatic	Count	0	3	0	3
	% of Total	0.0%	2.3%	0.0%	2.3%
Lymphoma	Count	0	0	2	2
	% of Total	0.0%	0.0%	1.6%	1.6%
Ependymal Tumor	Count	0	13	0	13
	% of Total	0.0%	10.2%	0.0%	10.2%
Total	Count	34	56	38	128
	% of Total	26.6%	43.8%	29.7%	100.0%

***Table No (8) Cross tabulation between the radiologist diagnosis of brain tumors* and PRESS and STRESS results**

Diagnosis	STEAM		Total	PRESS		Total
	Normal	Above		Normal	Under	
Astrocytoma	55	3	58	55	3	58
	42.9%	2.3%	45.3%	42.9%	2.3%	45.3%
Gliomatosis Cerebri/ GlioblasticMultiform/ (GBM)/and Oligodendroglioma	44	0	44	44	0	44
	34.4%	0.0%	34.4%	34.4%	0.0%	34.4%
Meningioma	6	2	8	6	2	8
	4.7%	1.6%	6.2%	4.7%	1.6%	6.2%
Metastatic	3	0	3	3	0	3
	2.3%	0.0%	2.3%	2.3%	0.0%	2.3%
Lymphoma	2	0	2	2	0	2
	1.6%	0.0%	1.6%	1.6%	0.0%	1.6%
Ependyal Tumor	13	0	1	13	0	13
	10.2%	0.0%	0.8%		0.0%	10.2
	123	5	128	123	5	128
	96.1%	3.9%	100.0 %	96.1%	3.9%	100.0 %
	P-value =0.042			P-value=0.042		

Table No (9): Descriptive Statistics of classification of lesions according to WHO grading, MRS metabolite and Radiologist MR imaging features of brain tumors.

Descriptive Statistics					
	N	Minimum Metabolite Value	Maximum Metabolite Value	Mean Metabolite Value	Std. Deviation
Benign (**G1**)	35	0.25	2.88	1.1591	.36675
Benign (**GII**)	13	1.50	2.25	1.8346	.24333
Malignant (**GIII**)	39	2.17	2.97	2.7997	.19250
Malignant (**GIV**)	39	2.88	6.38	3.7905	.98943

Table No (10) Distribution of study sample according to radiologist diagnosis

Diagnosis	Frequency	Percentages (%)
Astrocytoma (Pilocystic, Anaplastic and Diffused)	58	45.3
Gliomatosis Cerebri/ Glioblastic Multiform/ (GBM)/ Oligodedrogiomas	44	34.4
Meningioma	8	6.3
Metastatic	3	2.3
Lymphoma	2	1.6
Ependymal tumors	13	10.1
Total	128	100.0 (%)

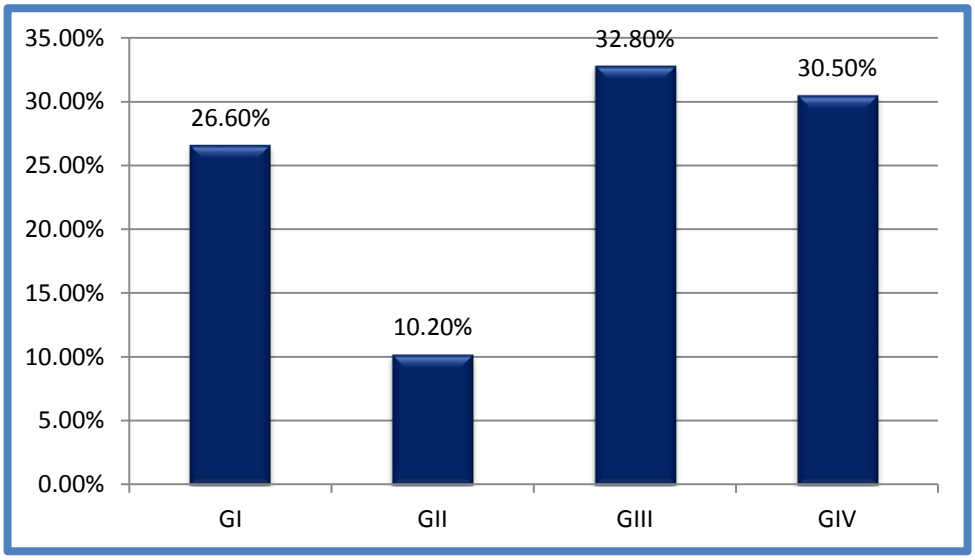

Figure No (1) Distribution of study sample according to Participant's tumors Grading

Table No (11) Mean age, gender distribution, metabolite ratio values, diagnosis-category of grading tumors {mean values} and radiologist diagnosis according to the standard criteria of Pilocystic, Anaplastic and Diffused Astrocytoma.

Mean age /Gender	**Metabolite Values**		**Diagnosis-category Grading tumors***				**Diagnosis**
			Benign		**Malignant**		
	Cho/ NAA	**Cho/ Cr**	**GI**	**GII**	**GIII**	**GIV**	
41.82±16.14 ***M=9,F=8***	1.12 ±0.17	1.38 ±0.39	1.17 ±0.14	-	-	-	Pilocystic Astrocytoma
53.0±14.98 **M=9,F=6**	1.85 ±0.80	2.68 ±0.43	-	-	2.79 ±0.10	3.01 ±0.0	Anaplastic Astrocytoma
43.34±15.57 **M=21, F=5**	2.19 ±1.26	2.87 ±0.57	-	-	2.75 ±0.0	3.51 ±0.32	Diffused Astrocytoma

Site of brain tumors were as follows : Both frontal lobes ,Insular cortex , Basal ganglia , Occipital lobe, ,RT frontal ,LT frontal ,RT temporal, LT temporal, Intra- axial , RT.Parietal-occipital, Fronto-temporal , Left cerebral hemisphere, Splenium of corpuscallosum, Hypothalamus, left cerebellar hemisphere , vermis and Thalamus

Table No (12) Mean age, gender distribution, Metabolite ratio Values, diagnosis-category of Grading tumors {mean values} and radiologist diagnosis according to the standard criteria of ependimal Tumors

	Metabolite Values		**Diagnosis-category of Grading tumors**				**Diagnosis**
			Benign		**Malignant**		
	Cho/ NAA	**Cho/ Cr**	**GI**	**GII**	**GIII**	**GIV**	
56±15.44 **F>M**	0.94	2.05	0.89	-	2.8	1.67	*Ependymal Giant Cell Astrocytoma
58.57±16.81 **M>F**	1.20 ±0.25	1.31 ±0.27	1.07 ±0.02	1.76 ±0.0	-	-	**Sub Ependymal Giant Cell Astrocytoma

*LT temporal, LT anterior horn of lateral ventricle, Occipital lobe. **RT Parietal, RT Frontal, Bi- frontal, LT orbital apex LT temporal and Thalamus.

Table No (13) Mean age, gender distribution, Metabolite Values, diagnosis-category of Grading tumors {mean values} and radiologist diagnosis according to the standard criteria of Glioblastic Multiform (GBM) Gliomatosis Cerebri and Oligodendroglioma

Mean age /Gender	**Metabolite Values**		**Diagnosis-Category Grading Tumors**				**Diagnosis**
			Benign		**Malignant**		
	Cho/NAA	**Cho/ Cr**	**GI**	**GII**	**GIII**	**GIV**	
42.72±15.14 **F= 11,M=13**	2.72 ±1.76	3.14 ±1.23	1.23	1.98	2.88	4.07 ±1.26	Glioblastic Multiform(GBM)
41.91±14.16 **F=3 ,M=6**	1.70 ±0.11	2.13 ±0.53	-	1.89 ±0.22	2.8	2.13 ±0.34	Gliomatosis Cerebri
47.62±12.11 **F=4, M=7**	1.74 ±0.82	3.19 ±0.26	-	-	2.88 ±0.02	3.93 ±0.00	Oligodendroglioma

Table No (14) Mean age, gender distribution, Metabolite Values, diagnosis-category of Grading tumors {mean values} and radiologist diagnosis according to the standard criteria of Meningioma, Lymphoma

Mean age /Gender	**Metabolite Values**		**Diagnosis-Category Grading Tumors**				**Diagnosis/site**
			Benign		**Malignant**		
	Cho/ NAA	**Cho/ Cr**	**GI**	**GII**	**GIII**	**GIV**	
M=4, F=4 49.63±15.98	1.26±0.33	2.08±0.88	1.09	1.5	2.87	3.21	**Meningioma** Extra-Axial, Under Flax
M=5 52.0±14.00		1.39 ±0.22	**1.08 ±0.18**		**1.23 ±0.19**		**Lymphoma** RT. Parietal-Occipital

Table No (15) Mean age, gender distribution, Metabolite ratio Values, diagnosis-category of Grading tumors {mean values} and radiologist diagnosis according to the standard criteria of Metastases

Mean age /Gender	**Metabolite Values**		**Diagnosis-Category Grading Tumors**				**Diagnosis/site**
			Benign		**Malignant**		
	Cho/ NAA	**Cho/ Cr**	**GI**	**GII**	**GIII**	**GIV**	
M =3 47±17.38	2.04 ±0.41	2.88 ±1.04		**2.13**	**2.5**	**2.97**	**Metastases** Intra- Axial

Table No (8) Metabolite Values, diagnosis-category of Grading tumors {mean values} and p- value

Grading	***NAA***	***Cho***	***Cr***	***Cho/ NAA***	***Cho/ Cr***	***NAA/ Cr***	***Lactate***	***Lipids***
GI	1.29 ±1.484	1.32 ±1.51	1.45 ±1.65	1.07 ±.224	1.43 ±.554	1.13 ±.262	1.70 ±.632	.94 ±.056
GII	0.77 ±.278	0.92 ±.340	1.00 ±.80	1.60 ±.292	2.07 ±.613	1.34 ±.697	1.23 ±.234	1.12 ±.311
GIII	0.96 ±.578	1.36 ±1.12	1.28 ±.988	1.78 ±.956	2.69 ±.498	1.40 ±.885	1.34 ±.258	.84 ±.110
GIV	0.64 ±.421	1.18 ±1.14	1.31 ±1.18	2.61 ±1.670	3.19 ±.935	1.22 ±.649	1.21 ±.285	1.06 ±.573
P-value	***.016***	***.696***	***.733***	***.000***	***.000***	***.509***	***.182***	***.801***

Chapter five

Discussion, Conclusion and Recommendation

Discussion, Conclusion and Recommendation

5.1 Discussion

5.1.1 Discussion of Diagnostic value of MRI and MRS in characterization of brain tumors

In our clinical practice we used for MRS : Long TE (1500/144ms) where the signal from most metabolites in the brain is lost except that of choline (Cho), creatine (Cr), N-acetyl aspartate (NAA), and lactate. Conversely, short TEs (2000/35ms) that allow for identification of many other metabolites Lipids, lactate, ala, myoinositol, glutamate, and glutamine. There is no enough studies are available concerning the application of Cho/Cr, and Cho/NAA ratios in studying the brain tumors with pathology related radiologist findings. This study provided a comparative evaluation of Cho/Cr, Cho/NAA ratios and pathological grade in the evaluation of brain tumors. Metabolite concentrations were detected and quantitatively analyzed by MRS.

Table No (9) showed descriptive statistics of classification of lesions according to WHO grading of, MRS metabolite and radiologist MR imaging features of brain tumors. Its ranges were 1.2±.37, 1.8±0.24, 2.8±0.19 and 3.8±0.99 for GI,GII,GIII, and GIV respectively where GIII and GIV were the most frequent in our sample as seen in figure (1)We classified the astrocytoma to as classified into (Pilocystic, Anaplastic and Diffused) and all were constituting 58 out of 128 cases ,Gliomatosis Cerebri/ Glioblastic Multiform/(GBM)/ Oligodedrogiomas constituting 44 cases Meningioma were 8, lymphoma were 2 ,Ependymal tumors were 13 and metastases were3cases out of 128 as presented in table (2)

Pilocystic Astrocytomas were diagnosed as GI which is low grade tumor demonstrated marked reduction of Cho/Cr comparing with anaplastic which were diagnosed as grade III and IV(3.01) ,and higher levels were found in diffused astrocytoma Grade III(3.51±0.32) as presented in table (3).

Studies showed that MRS can distinguishes normal brain tissues from astrocytomas (***Gill SS, et al***). However, it may not be able to distinguish between different histologic grades of malignancy in astrocytomas (***Fulham MJ, et al***). The typical MRS characteristics of astrocytomas include a significant reduction in NAA, a moderate reduction in Cr, and an elevation of Cho and Cho/ Cr (table8)making the Anaplastic Astrocytoma and diffused Astrocytoma to be categorized as malignant with GIII and GIV ,reduction of NAA probably indicates a loss of normal neuronal elements as they are destroyed and/or substituted by malignant cells, this was similarly what was mentioned by previous studies(***Fulham MJ, et al***) .Reduction of Cr is probably related to an altered metabolism, and elevation of Cho may reflect increased membrane synthesis and cellularity both of which are present in tumors (***Miller BL, et al***).Elevation of lactate may reflect tumor hypoxia.(***Ralph Weissleder, et al)*** Pilocystic Astrocytoma was found to be related to grade I.

Ependimal tumors were classified into ependymal giant cell astrocytoma which were classified in most of the cases to be grade I,III and IV and Sub Ependymal Giant Cell Astrocytoma were classified as GI and GII ,they affected both genders with similar age groups ,however in the literature

it was mentioned that Ependymoma are common in children and Subependymoma affected the older patients

but we found in our sample that the most affected ages were 56,58.57 years and ependimoma were more in female and the sub ependymoma were present more in males similarly it was mentioned that Subependymoma which is asymptomatic fourth ventricular tumor found in

elderly males (***Mauricio Castillo, et al***) 66% arise in the fourth ventricle; 33% in lateral ventricles, unlikely our current study found that it can affected any site within the brain

including the left temporal, left anterior horn of lateral ventricle, Occipital lobe. Right Parietal, Right Frontal, Bi- frontal, left orbital apex ,left temporal and Thalamus. Cho/ Cr showed higher values than subependimoma (table 4) Glioblastic Multiform (GBM) showed increased in Cho/NAA and Cho/ Cr as presented table(5)and considered as high grade tumors GIV followed by Oligodendroglioma then Gliomatosis Cerebri, as well all of these tumors have an increasing in lactate values as presented in table (8) .similarly Some investigators have proposed that the presence of lactate are correlated with a higher degree of malignancy and that it is commonly observed in glioblastoma multiform (***Demaerel P, et al***).Meningiomas were found Extra-Axial and Under Flax, with high values of Cho/ Cr and were considered to be as grade I,II, III and IV. The diagnosis of a meningioma was done with clear-cut from the MR images. meningiomas do not contain NAA because it arise outside the central nervous system (***Bruhim H, et al***).

The signal of Cho is markedly increased and the
Lactate and alanine are also elevated similar findings were observed in the previous studies (***Bruhim H***, ***Bunkege J***)
There is no clear explanation for the increase in alanine in meningioma(***Bunkege J,et al***).Some meningiomas, which invade the brain, show resonances in the location of NAA, which make the differentiation from astrocytomas difficult. Therefore the biopsy is important in those cases .Lymphoma was presented In 5 male patients at the right.
Parietal-Occipital region, and were classified as grade I and III tumors. In the presence of a lesion, differentiating between primary and secondary brain tumors is important but not frequently achievable. As well MRS findings are also unclear in this situation where it was diagnosed as GII, GIII, and GIV with high Cho/ Cr and Cho/ NAA similar results have been mentioned in previous studies (***Demaerel P, Ott D***).
Metastases show reduction of NAA, a decreased Cr signal, and elevated Cho these features are similar to astrocytomas we have justified the difficulties in diagnosis the metastes is that some metastases may also contain lipids [28] and the Lipid is present in high-grade astrocytomas, therefore Metastases to the brain become as difficult burden to the radiologists in the differentiation between metastases and astrocytoma.
The mean values for normal NAA/Cr, Cho/Cr, and NAA/Cho ratios were 1.44, 0.66 and 2.20 respectively. (***Ott D, et al***)

In tumors, Cho levels increase from G II and G III because of increased membrane synthesis and proliferation, while NAA levels fall from 0.96±.578 in grade 3to grade 4 (0.64±.42) because neurons and axons are impaired and destroyed ,the same justification was mentioned in previous study done by (***Sijens PE,et al***).

There is also a fall in Cr levels in tumors in GI and GII ,GIII and IV because of energy exhaustion and rise in lipids from necrosis as mentioned by [30].The presence of lipid or lactate resonances in the MR spectra was not predictive for tumor growth with no significant relation between the grading and the values of lactate and lipids (p= 0.182 and 0.801) as presented in table (8) the justification is that necrosis can resulted from tumor progression and therefore they could not be used for the differentiation of lesions similarly previous studies have mentioned that (***Fulham MJ, Miller BL, Ralph Weissleder, Miller BL***).Results of this study showed that grade IV tumor had mean Cho/NAA and Cho/Cr ratios higher than grade III and ratios were two times higher than ratios of grade I or II. This were significantly correlated in tumor grading at p=0.000 and 0.000 respectively.

The predictable metabolite concentrations accounted in this study were, in agreement with the prior literature values (***Fulham MJ, Miller BL, Ralph Weissleder***).In grade IV, the mean Cho/NAA and Cho/Cr ratios in this study were 2.61±1.670 and 3.19±.935 respectively. In grade 3 tumors, ratios were 1.78 ±.956and 2.69 ±.498 respectively, while in grade II tumors, the ratios were 1.60 ±.292and 2.07 ±.613respectively.

In grade I astrocytoma, ratios were 1.07±.224 and 1.43±.554 respectively, so grade 4 tumors had the highest ratios and the grade I astrocytoma had the lowest and was proved to be correlated significantly at p= 0.000 and 0.000 (table8).Ratios higher than 1.5 for either Cho/Cr or Cho/NAA were diagnostic of tumor and ratios higher than 2 were suggestive of high grade glioma.

This agrees with ***(Weybright et al.)*** NAA, Cho, Cr, NAA/ Cr, Lactate and Lipids metabolic values alone showed no significant relation between the values to be increased or decreased according to grading therefore the dependency of grading should be based upon the Cho/ NAA and Cho/ Cr .From this account and metabolic ratios it was suggested to diagnose, differentiate and grade gliomas after evaluating the Cho/ NAA and Cho/ Cr.

5.1.2 Discussion of Grading of Brain Tumors using MR Spectroscopy: Diagnostic value at Short and Long TE

The study was designed by obtaining a spectrum, that was analyzed, and was influenced by many parameters, including chemical characteristics of each metabolite and the compounds in which they are located; NAA ,Cho, Cr Cho/ NAA, Cho/ Cr, NAA/ Cr , Lactate and Lipid at the selection of the area to study. Lesions to be considered are cystic, solid, homogeneous, and heterogeneous. And the perfusion character to be as hyper-perfusion, normal and hypo- perfused. Choice of the technique type to be employed was (monovoxel or multivoxel) and

of the sequence to be used (PRESS and STEAM) and the choice of the echo time (short or long). Table (1) presented the distribution of the sample age; the most common affected age was age between 41-50 years old constituting 34(26.6%).Table (2) showed detailed distribution of tumor territory in the brain site cross tabulated with age where a significant relation was detected between the site and age at p-value= 0.006**.**

All the lesion were diagnosed according to the standard criteria of diagnosis done by radiologist, the astrocytomas, were found in 58(45.3%) of the cases where the ependymoma and lymphoma were found in 13(10.1%) and 2(1.6%) of the cases in respectively (table 3) Classification of astrocytoma is divided basically into Fibrillary astrocytomas including Astrocytoma, WHO grade I (AI), Astrocytoma, WHO grade II (AII),Anaplastic astrocytoma, WHO grade III (AA III), Glioblastoma multiforme, WHO grade IV (GBM IV), and Other astrocytomas: Gliomatosis cerebri, Pilocytic astrocytoma ,Giant cell astrocytoma ,sub ependymal tumor and other types(***Lukasa , L.D., et al 2005***). In our sample the astrocytoma included (diffused anaplastic ,Glioblastoma multiforme , Pilocytic astrocytoma and giant cell astrocytoma and are constituting most of the cases 58 out of 128 (45.3%).Anaplastic astrocytomas are mostly located in the cerebral hemispheres with imaging features as heterogeneous mass with edema appears in most of the cases with good enhancement after contrast .Glioblastoma multiforme (GBM) also was located is in the hemispheres with imaging features appears as heterogeneous mass highly contrast enhancement with extensive vasogenic edema and mass effect.

The Pilocytic astrocytomas appear in the cerebellum and are usually appear as cystic and have intense mural enhancement. Gliomatosis cerebri was found in 44(34.4%) of the cases and is characterized as diffuse growth of glial neoplasm within brain, with no gross mass lesions but a diffuse infiltration of brain tissue by tumor cells are present; it appears as non-enhancing lesions. Ependymal tumors were found to be 13(10.1%) out of the 128 case, 5 cases were Ependymoma and 8 were Subependymoma, it was located adjacent to ventricles within the parenchyma and periventricular area with imaging features resemble astrocytoma . Our trend in the classical diagnosis depend upon the T1 and T1 after contrast it allows differentiation of lesions by the difference in the standard criteria of diagnosis and signal intensity (***Lukasa , L.D., et al 2005***) .The current study used the perfusion technique and were characterized as moderate ,poor and well perfused ,this was noticed in table(4). Because conventional MRI allows for only indistinguishable identification and localization of tumors, biopsies were routinely required to diagnose tumors. Unfortunately, many tumors may be unapproachable for biopsy; therefore another method is needed. MRS had the advantage of being a noninvasive diagnostic procedure. ***(Carles,M.S, et al2004,Margan,H.,et al 2010***) For that reason we investigate the value of this technique in diagnoses of brain tumors by comparing the radiologist reports at perfusion ,STEAM and PRESS with the MRS chemical results, Table No (5) . Studies showed that MRS can show the abnormal findings in nearly 100% of brain tumors, as well it is useful in the differential diagnosis of brain tumors and in characterization of metabolic changes associated with tumor progression,

degree of malignancy, and response to treatment ***(Louis,D.N., et al 2001-Fullham,M,J. et al1992)*** At present study, the best possible pulse sequence parameters when using MRS for characterizing tumors are controversial. The parameter that largely influences the spectrum is TE. A long TE allows the observation of a reduced number of metabolites and has less baseline distortion, yielding a spectrum that is easy to process, analyze, and interpret. At approximately 144 TE, Ala and Lactate doublets are inverted because of J-coupling, making it easier to differentiate these resonances from lipids and other molecules. On the other hand, more resonances are visible at short TE because the signal intensity from compounds with strong J-modulation may be lost at long TE. Accordingly, a short TE is used for better evaluation of lipids, myo-inositol, glutamine, and glutamate. In this study, we tested the influence of TE; Long TE (1500/144) and Short TE (2000/35) in the classification of the most common tumor types found in the brain. In Normal spectroscopy Cho/Cr ratio is near 1; ratio 2:1 and in high grade tumors decreased NAA Cho/Cr ratio > 2:1 (***Lukasa , L.D., et al 2005***) and in cases of brain tumors it showed multiple metabolic changes including high Cho ,low NAA, low Cr, high Lactate and Lipids.[24] Diffusion-weighted imaging provides a way to evaluate the diffusion properties of water molecules in tissue and has been used for diseases ***(Miller, L.,et al1991)*** A review In recent publications, diffusion-weighted imaging is believed to be valuable in the diagnosis of different lesions and tumors. ***(Castillo,L.S., et al 1996, Demaerel, C.L, et al2002).*** The current study was obtained to compare MRS findings with those of diffusion-weighted imaging to determine which technique is more effective in characterization and diagnosis of brain tumors.

The current study showed significant results between the perfusion findings and the MRS values regarding Cho/ NAA 1.83±1.224 at p= (0.000) and Cho/ Cr value 2.45±.968 at p = (.000) with no significant relation between other MRS parameters with STEAM and PRESS techniques.

In our clinical practice we used short echo times (TEs) less than 30ms and adequate scan was obtained with TE as long as 144ms and 288ms milliseconds for PRESS technique. For MRS using Long TE (1500/144ms); the signal from most metabolites in the brain is lost except that of choline (Cho), creatine (Cr), N-acetyl aspartate (NAA), and lactate. Conversely, short TEs (2000/35ms) allow for identification of many other metabolites Lipids, lactate, ala, myoinositol, glutamate, and glutamine. For this important value, MRS is better to be included as part of a routine imaging study. At our institution, we have created a set organized work which allows the technologist to perform the study easily by setting the location of the voxel and tailoring its size to correspond grossly to the abnormality in question. A voxel should include as much of the abnormality as possible and little normal surrounding brain tissue. Astrocytomas show a relative reduction in NAA and Cr, and Cho comparing with the lymphoma .The spectra of metastases are similar to those of meningioma and gliomatos cerebri and ependemal tumors, with low NAA, low Cr, and high Cho levels. The difference was found to be significant in the NAA values at different brain lesions with no significant value in the reduction or increasing of Cho and Cr these were noticed in table (6) Similarly; regarding astrocytomas, several studies, have suggested an association between tumor character and Cho levels,

the higher grade tumors having greater Cho concentrations***. (Sijens, P.M, et al 1994)*** Some studies have found high-grade tumors glioblastoma multiforme (GBM)) to have lower levels of Cho than grade II or grade III astrocytoma This may be due to the presence of necrosis in high-grade tumors, particularly those with necrotic cores, since necrosis is associated with low levels of all metabolites.(***Hemminghaus, S., et al 2003– Magalhaes , A. G., et al 2005- Schlemmer,H.P, B., et al 2001)*** Our opinion is that tumors are commonly heterogeneous, with necrotic cores, proliferative rims and invasion of surrounding brain tissue and the spectrum may vary greatly depending on the region that is sampled by MRS therefore, the region-of interest chosen for analysis may have a large influence on the results. One study used MR perfusion imaging to guide the spectral measurement location; and they found no significant relation between changes in NAA,Cho,Cr, Cr, NAA/Cr, lactate and lipids were detected in normal or hypo perfused tumor regions while the Cho/NAA and Cho/Cr has significant impact [33] But our study showed a significant relation between the diagnosis and the character of the tumors to be hyper or hypo or normal perfusion as noticed in table(7) The current study results was consistent with previous studies (***Weybright P,,et al 2005- Shokry ,et al 2012)*** who have mentioned that for characterization of metastases from other brain tumors, it has been suggested that gliomas showed elevation in Cho in surrounding tissue where metastatic lesions tend to be more encapsulated and therefore show high Cho signals or other abnormalities outside the region of enhancement as well metastatic lesions always elevated lipid peaks;

thus, if the lesion does not exhibit mobile lipid signals, anaplastic glioma is more likely.

The current study showed that Cho/Cr has significant impact in differentiation of lymphoma from other lesions with p value = 0.004 where the other parameters Cho/ NAA, NAA/ Cr, Lactate and Lipid have no significant relationship.

By combining both MRS and perfusion MRI, the diagnosis of lesions was achieved with value of 0.944±.896 for NAA and Cho/ NAA 1.83±1.224 however another study showed that the cutoff points of NAA/Cho ≤ 0.61 and rCBV ≥1.50 in corresponding to tumor diagnosis.[37] and another one showed that presence of tumor was indicated when Cho/NAA ratio was greater than 1.9***(Arnold ,D.L1, et al 1994)*** .Table (7,8) showed a significant relation between the diagnosis of tumors and Perfusion-MRI (rCBV) , STEAM and PRESS results at P-value=0.001,0042 and 0.042 in respectively.

5.2 Conclusion

The diagnostic strategy was evaluated; Perfusion-MRI (rCBV) and MRS are useful as additional imaging techniques for establishing the differential diagnosis between brain metastases and brain tumors. Both has significant relation in differentiation and diagnosis of brain tumors; as hyper-hypo or normally perfused as well in chemical characteristics of each metabolite and the compounds in which they are located; N-acetyl aspartate (NAA) , Cho/ NAA, Cho/ Cr at the selection of the area to study. MRI-based techniques including results from perfusion MRI, and MRS were proposed to improve the diagnosis and characterizing of brain lesions as astrocytoma, Gliomatosis cerebri ,meningioma, lymphoma ,ependymal tumors and metastases.

Long TE of (1500/144ms) where the signal from most metabolites in the brain is lost except that of choline (Cho), creatine (Cr), N-acetyl aspartate (NAA), and lactate and short TEs of (2000/35ms) those allow for identification of many other metabolites Lipids, lactate, ala, myoinositol, glutamate, and glutamine were used.

MRS metabolic ratios (Cho/Cr and Cho/NAA) can be used to grade and differentiate gliomas. Ratios less than 1.5 were suggested to be in necrotic or normal brain tissue; ratios from 1.5 to 2 were suggested to be as low grade glioma and ratios higher than 2 were suggested to be high grade glioma or metastasis. Metastases were similar to high grade glioma in its readings .Meningioma can be diagnosed by MRI images. MRS should added to routine MR imaging studies as it provides greater information concerning tissue characterization than what is possible with MR imaging studies alone

5.3 Recommendation

1. To use both MRI,MRS and perfusion to diagnosis and characterize brain tumor
2. To use single voxel and multivoxel while studding MRS for full studies to cover the result while biopsy for the study the accuracy of MRS

Appendices

Appendix (I)

Data collection sheet(1)

Patients		Tumor territory in the brain			T1 weighted TR< 500ms TE< 50ms		T2weighted TR> 1500ms TE> 80ms		MRI with contrast in T1 weighted image		Nullifying the signal from CSF		Perfusion MRI (rCBV)		STEAM	PRESS		
Sex	Age																	
					Anatomy		Pathology		Tumor									

Appendix (II)

Detail Data collection for each sample

patients		Tumor territory in the brain	Conventional MRI	T_1weighted TR < 500ms TE < 50ms	T_2weighted TR >1500ms TE >80ms	MRI with contrast in T_1weighted image	Nullifying the Signal from CSF	Change in blood O_2 level	STEAM	PRESS	Biochemistry of the tumor							
Sex	Age								TE< 30ms TE = 144ms SVS	Spin echo sequences TE = 144ms 288ms	long TE (1500/144)			Short TE (2000/35)				
				Anatomy	Pathology	**Tumors or infections**					NAA	Cho	Cr	Lip	Lac	Glx	MI	Ala
1/ M/27		Both frontal	Done	Abnormal	Present	Tumor	Done	Done	Done	Done	**0.67**	**0.73**	**0.67**	*	*	*	*	*
2/ M /50		L.Temporal	Done	Abnormal	Present	Tumor	Done	Done	Done	Done	**0.98**	**2.2**	**0.99**	**1.6**	**0.98**	*	*	*
3/ F /45		R. Parietal	Done	Abnormal	Present	Tumor	Done	Done	Done	Done	**0.18**	**1.15**	**0.41**	*	*	*	*	*
4/F/55		R.Parietal	Done	Abnormal	Present	Tumor	Done	Done	Done	Done	**0.59**	**1.72**	**0.61**	*	*	*	*	*
5/ M /54		L. Frontal	Done	Abnormal	Present	Infection	Done	Done	Done	Done	**0.35**	**1.01**	**0.90**	*	*	*	*	*
6/ F /39		Extra-axial	Done	Abnormal	Present	Tumor	Done	Done	Done	Done	*	*	*	**1.4**	**0.97**	**2.4**	*	*
7/ M /57		R.Parietal-occipital	Done	Abnormal	Present	Infection	Done	Done	Done	Done	**1.56**	**3.9**	**0.78**	**1.3**	**0.96**	*	*	*
8/ M /49		R. Temporal	Done	Abnormal	Present	Infection	Done	Done	Done	Done	**1.6**	**3.7**	**3.05**	**1.7**	**1.45**	*	*	*
9/ M /70		Extra-axial	Done	Abnormal	Present	Infection	Done	Done	Done	Done	**1.48**	**3.9**	**3.11**	**2.10**	**1.57**	*	*	*
10/ M / 38		L. Parietal	Done	Abnormal	Present	Tumor	Done	Done	Done	Done								
11/ M /66		R.Parietal-occipital	Done	Abnormal	Present	Tumor	Done	Done	Done	Done								
12/ F /43		L. Parietal	Done	Abnormal	Present	Tumor	Done	Done	Done	Done								
13/ F / 36		L. Frontal	Done	Abnormal	Present	Tumor	Done	Done	Done	Done								
14/ M /69		R. Frontal	Done	Abnormal	Present	Infection	Done	Done	Done	Done								
15/ M /48		Occipital	Done	Abnormal	Present	Infection	Done	Done	Done	Done								
16/ M /57		Intra- axial	Done	Abnormal	Present	Tumor	Done	Done	Done	Done								
17/ M /29		R.forantal	Done	Abnormal	Present	Tumor	Done	Done	Done	Done								
18/ M/46		L.Temporal	Done	Abnormal	Present	Tumor	Done	Done	Done	Done								
19/ F / 60		Occipital	Done	Abnormal	Present	Tumor	Done	Done	Done	Done								
20/ M /49		Basal ganglia	Done	Abnormal	Present	Infection	Done	Done	Done	Done								
21/ F /83		Bilateral	Done	Abnormal	Present	Tumor	Done	Done	Done	Done								

Appendix (III)

Publication

Final Sabri onlineM1609087280.pdf

98d8d8336cef7a981c239803265eee24c7ce.pdf

To open the published paper please double click mouse with index and print the 2 papers

Please rearrange the References in alphabetic manner

References :

1- Magalhaes A, Godfrey W, Shen Y, et al.. Proton magnetic resonance spectroscopy of brain tumors correlated With pathology.Acad Radiol 2005;12:51–7.

2- Herminghuas S, Dierks T, Pilatus U, et al.. Determination of histopathological tumor grade in neuroepithelial brain tumors by using spectral pattern analysis of in vivo spectroscopic data. J. Neurosurg 2003;98:74–81.

3- Lau DW, Klein NC, Cunha BA. Brain abscess mimicking brain tumor. *Heart Lung* 1989;18:634–637

4- Mamelak AN, Mampalam TJ, Obana WG, Rosenblum ML. Improved management of multiple brain abscesses: a combined surgical and medical approach. *Neurosurgery* 1995;36:76–85

5- Demaerel P, Van Hecke P, Van Oostende S, et al. Bacterial metabolism shown by magnetic resonance spectroscopy. *Lancet* 1994;344:1234–1235

6- Harada M, Tanouchi M, Miyoshi H, Nishitani H, Kannuki S. Brain abscess observed by localized proton magnetic resonance spectroscopy.*Magn Reson Imaging* 1994;12:1269–1274

7- Remy C, Grand S, Lai ES, et al. 1H MRS of human brain abscess in vivo and in vitro. *Magn Reson Med* 1995;34:508–514

8- Ping H. Lai, Jih T. Ho, Wei L. Chen, Shu S. Hsu, Jyh S. Wang, Huay B. Pan, and Chien F. Yang 2004;31:73–89.Brain Abscess and Necrotic Brain Tumor:Discrimination with Proton MR Spectroscopy and Diffusion-Weighted Imaging *AJNR Am J Neuroradiol* 23:1369–1377, September 2002

9- Barker PB, Glickson JD, Bryan N. In vivo magnetic resonance spectroscopy of human brain tumors. *Top Magn Reson Imaging* 1993;5:32–45

10- Arnold DL, Shoubridge EA, Villemure JG, Feindel W. Proton and phosphorous magnetic resonance spectroscopy of human astrocytomas in vivo: Preliminary observations on tumor grading. *NMR Biomed* 1990;3:184–189

11- Bruhn H, Frahm J, Gyngell ML, et al. Noninvasive differentiation of tumors with use of localized 1H MR spectroscopy in vivo: initial experience in patients with cerebral tumors. *Radiology* 1989;172: 541–548

12- Herholz K, Heindel W, Luyten PR, et al. In vivo imaging of glucose consumption and lactate concentration in human gliomas. *Ann Neurol* 1992;31:319–327

13- Ott D, Hennig J, Ernst T: Human brain tumors: assessment with in vivo proton MR spectroscopy. *Radiology* 1993;186:745–752

14- Floeth FW, Stummer W. The value of metabolic imaging in diagnosis and resection of cerebral gliomas. Nat Clin Pract Neurol 2005;1:62–3.

15- Lukasa L, Devosa A, Suykensa JAK. Brain tumor classification based on long echo proton MRS signals. Artif Intell Med

16- Carles Majo´s, Margarida Julia`-Sape´, Juli Alonso, Marta Serrallonga, Carles Aguilera,Juan J. Acebes, Carles Aru´s, and Jaume Gili,Brain Tumor Classification by Proton MR Spectroscopy: Comparison of Diagnostic Accuracy at Short and Long TE *AJNR Am J Neuroradiol* 25:1696–1704, November/December 2004

17- Imaging of Brain Tumors: MR Spectroscopy and Metabolic ImagingAlena Horská, Ph.D.1 andUniversity School of Medicine, and The Kennedy Krieger Institute, Baltimore, MarylandPeter B. Barker, D. Phil.2Russell H Morgan Department of Radiology and Radiological Science, Johns Hopkins Neuroimaging Clin N Am. 2010 August ; 20(3): 293–310. doi:10.1016/j.nic.2010.04.003

18- Louis DN, Holland EC, Cairncross JG (2001) Glioma classification: a molecular reappraisal. Am J Pathol 159:779. Retrieved from http://www.ncbi.nlm.nih.gov/pmc/articles/PMC1850454/

19- Brandao L, Domigues R (2003). MR Spectroscopy of the Brain, Lippincott Williams & Wilkins. http://www.amazon.com/Spectroscopy-Brain-Lara-Brand-227/dp/0781746167/ref=sr_1_1?s=books&ie=UTF8&qid=1407910432&sr=1&keywords=MR+Spectroscopy+of+the+Brain.+Lippincott+Williams+%26+Wilkins%2C+2003

20- Garnett MR, Blamire AM, Corkill RG, et al.. Early proton magnetic resonance spectroscopy in normal-appearing brain correlates with outcome in patients following traumatic brain injury. Brain 2000;123:2046–54.
21- Gill SS, Thomas DG, Van Bruggen N, et al. Proton MR spectroscopy of intracranial tumors: in vivo and in vitro studies. *J Comput Assist Tomogr* 1990;14:497–504
22- Kugel H, Heindel W, Ernestus RI, Bunke J, du Mesnil R, Friedmann G. Human brain tumors: spectral patterns detected with localized H-1 MR spectroscopy. *Radiology* 1992;183:701–709
23- . Fulham MJ, Bizzi A, Dietz MJ, et al. Mapping of brain tumor metabolites with proton MR spectroscopic imaging: clinical relevance.*Radiology* 1992;185:675–686
24- . Miller BL. A review of chemical issues in 1H NMR spectroscopy: *N*-acetyl-L-aspartate, creatine, and choline. *NMR Biomed* 1991;4:47–52
25- Ralph Weissleder, Jack Wittenberg, Mukesh G. Harisinghani, John W. Chen, Boston, MassachusettsPrimer of*Diagnostic Imaging* FIFTH EDITIONCopyright © 2011 by Mosby, Inc., an affiliate of Elsevier Inc
26- Mauricio Castillo, Lester Kwock, and Suresh K. Mukherji Clinical Applications of Proton MR Spectroscopy AJNR 17:1–15, Jan 1996
27- Demaerel P, Johannik K, Van Hecke P, et al. Localized H-1 NMR spectroscopy in fifty cases of newly diagnosed intracranial tumors.*J Comput Assist Tomogr* 1991;15:67–76
28- . Sijens PE, van Dijk P, Oudkerk M. Correlation between choline level and Gd-DTPA enhancement in patients with brain metastasesof mammary carcinomas. *Magn Reson Med* 1994;32:549– 555
29- Nelson SJ. Multivoxel magnetic resonance spectroscopy of brain tumors. Mol Cancer Ther 2003;2:497–507.
30- Herminghuas S, Dierks T, Pilatus U, et al.. Determination of histopathological tumor grade in neuroepithelial brain tumors byusing spectral pattern analysis of in vivo spectroscopic data. J. Neurosurg 2003;98:74–81.
31- Magalhaes A, Godfrey W, Shen Y, et al.. Proton magnetic resonance spectroscopy of brain tumors correlated With pathology.Acad Radiol 2005;12:51–7.
32- Schlemmer HP, Bachert P, Herfarth KK, et al.. Proton MR spectroscopic evaluation of suspicious brain lesions after stereotactic radiotherapy. AJNR 2001;22:1316–24.
33- Ahmed ShokryMRS of brain tumors: Diagrammatic representations and diagnostic approach The Egyptian Journal of Radiology and Nuclear Medicine (2012) 43, 603–612

34- Weybright P, Sundgren PC, Maly P, et al.. Differentiation between brain tumor recurrence and radiation injury using MR spectroscopy. AJR 2005;158:1471–6.
35- Ahmed Shokry(2012) MRS of brain tumors: Diagrammatic representations and diagnostic approachThe Egyptian Journal of Radiology and Nuclear Medicine 43, 603–612.
36- Alena Horská, Peter B. Barker, D. Phil. 2010 Imaging of Brain Tumors: MR Spectroscopy and Metabolic Imaging Neuroimaging Clin N Am. August ; 20(3): 293–310.
37- Andreasen NC (1988) Brain imaging: applications in psychiatry. Science 239:1381-1388. Retrieved from http://www.brainmapping.org/ NITP/PNA/ Readings/ Andreasen1988.pdf
38- Arnold DL, Shoubridge EA, Villemure JG, Feindel W. Proton and phosphorous magnetic resonance spectroscopy of human astrocytomas in vivo: Preliminary observations on tumor grading. NMR Biomed 1990;3:184–189
39- Atlas SW (2009) Magnetic resonance imaging of the brain and spine. Vol. 1, Lippincott Williams & Wilkins. Retrieved from http://books.google.com/books?hl=en&lr=&id=Mu7MmTXkPeAC&oi=fnd&pg=PA2&dq=Magnetic+Resonance+Imaging+of+the+Brain+and+Spine+&ots=r-HF5m9Ljk&sig=4kyZ3_v7isCJ_RucvOLgI4voALo
40- Barker PB, Glickson JD, Bryan N. In vivo magnetic resonance spectroscopy of human brain tumors. Top Magn Reson Imaging 1993;5:32–45

41- Barker PB, Lee RR, McArthur JC (1995) AIDS dementia complex: evaluation with proton MR spectroscopic imaging. Radiology 195:58-64. Retrieved from http://pubs.rsna.org/doi/abs/10.1148/radiology.195.1.7892496
42- Bottomley PA. Spatial localization in NMR spectroscopy in vivo. Ann N Y Acad Sci 1987;508:333–348. [PubMed: 3326459]
43- Brandao L, Domigues R (2003). MR Spectroscopy of the Brain, Lippincott Williams & Wilkins. http://www.amazon.com/Spectroscopy-Brain-Lara-Brand-227/dp/0781746167/ref=sr_11?s=books&ie=UTF8&qid=1407910432&sr=1-1&keywords=MR+Spectroscopy+of+the+Brain.+Lippincott+Williams+%26+Wilkins%2C+2003
44- Brant WE, Helms CA (1999) Fundamentals of diagnostic radiology. Lippincott Williams & Wilkins. Retrieved from http://books.google.com/books?hl=en&lr=&id=o_4eoeOinNgC&oi=fnd&pg=PP2&dq=Fundamentals+of+Diagnostic+Radiology&ots=mmWiwMw7XB&sig=XsHaiOG23xGMoYnHaLU4C8OPad4
45- Brown TR, Kincaid BM, Ugurbil K. NMR chemical shift imaging in three dimensions. Proc Natl Acad Sci U S A 1982;79(11):3523–3526.
46- Bruhn H, Frahm J, Gyngell ML, et al. Noninvasive differentiation of tumors with use of localized 1H MR spectroscopy in vivo: initial experience in patients with cerebral tumors. Radiology 1989;172: 541–548
47- Bushong CS (1996) Magnetic resonance imaging, 2nd edn. Retrieved from http://www.amazon.com/Magnetic-Resonance-Imaging-Biological-Principles/dp/0815113420/ref=sr_1_10?s=books&ie=UTF8&qid=
48- Butzen J, Prost R, Chetty V, et al. Discrimination between neoplastic and nonneoplastic brain lesions by use of proton MR spectroscopy: the limits of accuracy with logical regression model. AJNR Am J Neuroradiol 2000;21:1213–1219
49- Carles Majo´s, Margarida Julia`-Sape´, Juli Alonso, Marta Serrallonga, Carles Aguilera,Juan J. Acebes, Carles Aru´s, and Jaume Gili,Brain Tumor Classification by Proton MR Spectroscopy: Comparison of Diagnostic Accuracy at Short and Long TE AJNR Am J Neuroradiol 25:1696–1704, November/December 2004
50- Chang L, McBride D, Miller BL et al (1995) Localized in vivo 1H magnetic resonance spectroscopy and in vitro analyses of373. Retrieved from http://onlinelibrary.wiley.com/doi/10.1002/mrm.1910310404/abstract heterogeneous brain tumors. J Neuroimaging 5:157-163. Retrieved from http://europepmc.org/abstract/med/7626823
51- Chawla S, Wang S, Wolf RL, et al. Arterial spin-labeling and MR spectroscopy in the differentiation of gliomas. AJNR Am J Neuroradiol 2007;28(9):1683–1689.
52- Chiang IC, Kuo YT, Lu CY, et al. Distinction between high-grade gliomas and solitary metastases using peritumoral 3-T magnetic resonance spectroscopy, diffusion, and perfusion imagings. Neuroradiology 2004;46(8):619–627.
53- Demaerel P, Johannik K, Van Hecke P, et al. Localized H-1 NMR spectroscopy in fifty cases of newly diagnosed intracranial tumors.J Comput Assist Tomogr 1991;15:67–76
54- Demaerel P, Van Hecke P, Van Oostende S, et al. Bacterial metabolism shown by magnetic resonance spectroscopy. Lancet 1994;344:1234–1235

55- Desprechins B, Stadnik T, Koerts G, Shabana W, Breucq C, Osteaux M. Use of diffusion-weighted MR imaging in differential diagnosis between intracerebral necrotic tumors and cerebral abscesses. AJNR Am J Neuroradiol 1999;20:1252–1257
56- Dowling C, Bollen AW, Noworolski SM, et al. Preoperative proton MR spectroscopic imaging of brain tumors: correlation with histopathologic analysis of resection specimens. AJNR Am J Neuroradiol 2001;22:604–612
57- Fan G, Sun B, Wu Z, et al. In vivo single-voxel proton MR spectroscopy in the differentiation ofhigh-grade gliomas and solitary metastases. Clin Radiol 2004;59(1):77–85.
58- Floeth FW, Stummer W. The value of metabolic imaging in diagnosis and resection of cerebral gliomas. Nat Clin Pract Neurol 2005;1:62–3.
59- Frahm J. Localized Proton Spectroscopy using stimulated echoes. J Magn Reson 1987;72(3):502–508.
60- Fulham MJ, Bizzi A, Dietz MJ, et al. Mapping of brain tumor metabolites with proton MR spectroscopic imaging: clinical relevance.Radiology 1992;185:675–686
61- Garnett MR, Blamire AM, Corkill RG, et al.. Early proton magnetic resonance spectroscopy in normal-appearing brain correlates with outcome in patients following traumatic brain injury. Brain 2000;123:2046–54.
62- Gill SS, Thomas DG, Van Bruggen N, et al. Proton MR spectroscopy of intracranial tumors: in vivo and in vitro studies. J Comput Assist Tomogr 1990;14:497–504
63- Gillies RJ, Morse DL (2005) In vivo magnetic resonance spectroscopy in cancer. Annu Rev Biomed 7:287-326. Retrieved from http://www.gruporessonar.com. br/k/artigos/8033527.doc
64- Graves EE, Nelson SJ, Vigneron DB et al (2001) Serial proton MR spectroscopic imaging of recurrent malignant gliomas after gamma knife radiosurgery. AJNR Am J Neuroradiol 22:613-624. Retrieved from http://www.ajnr.org/content /22/4/613.full
65- Harada M, Tanouchi M, Miyoshi H, Nishitani H, Kannuki S. Brain abscess observed by localized proton magnetic resonance spectroscopy.Magn Reson Imaging 1994;12:1269–1274
66- Herholz K, Heindel W, Luyten PR, et al. In vivo imaging of glucose consumption and lactate concentration in human gliomas. Ann Neurol 1992;31:319–327
67- Herminghuas S, Dierks T, Pilatus U, et al.. Determination of histopathological tumor grade in neuroepithelial brain tumors by using spectral pattern analysis of in vivo spectroscopic data. J. Neurosurg 2003;98:74–81.
68- Hourani R, Horska A, Albayram S, et al. Proton magnetic resonance spectroscopic imaging to differentiate between nonneoplastic lesions and brain tumors in children. J Magn Reson Imaging 2006;23(2):99–107.
69- Hourani R, Brant LJ, Rizk T, et al. Can proton MR spectroscopic and perfusion imaging differentiate between neoplastic and nonneoplastic brain lesions in adults? AJNR Am J Neuroradiol 2008;29(2):366–372. [PubMed: 18055564]
70- Howe FA, Barton SJ, Cudlip SA, et al. Metabolic profiles of human brain tumors using quantitative in vivo 1H magnetic resonance spectroscopy. Magn Reson Med 2003;49(2):223–232.
71- Imaging of Brain Tumors: MR Spectroscopy and Metabolic ImagingAlena Horská, Ph.D.1 andUniversity School of Medicine, and The Kennedy Krieger Institute, Baltimore, MarylandPeter B. Barker, D. Phil.2Russell H Morgan Department of Radiology and Radiological Science, Johns Hopkins Neuroimaging Clin N Am. 2010 August ; 20(3): 293–310.

72- Ishimaru H, Morikawa M, Iwanaga S, et al. Differentiation between high-grade glioma and metastatic brain tumor using single- voxel proton MR spectroscopy. Eur Radiol 2001;11(9):1784– 1791.
73- Janet Cochrane Miller 2012 Magnetic Resonance Spectroscopy in the Brain volume 10issue 7
74- Kimura T, Sako K, Gotoh T, Tanaka K, Tanaka T. In vivo singlevoxel proton MR spectroscopy in brain lesions with ring-like enhancement. NMR Biomed 2001;14:339–349
75- Kugel H, Heindel W, Ernestus RI, Bunke J, du Mesnil R, Friedmann G. Human brain tumors: spectral patterns detected with localized H-1 MR spectroscopy. Radiology 1992;183:701–709
76- Lau DW, Klein NC, Cunha BA. Brain abscess mimicking brain tumor. Heart Lung 1989;18:634–637
77- Law M, Cha, Knopp EA, Johnson G, Arnett J, Litt AW (2002) High-Grade Gliomas and Solitary Metastases: Differentiation by Using Perfusion and Proton Spectroscopic MR Imaging Radiology 222:715-721.
78- Louis DN, Holland EC, Cairncross JG (2001) Glioma classification: a molecular reappraisal. Am J Pathol 159:779. Retrieved from http://www.ncbi.nlm.nih.gov/ pmc/articles/PMC1850454/
79- of chemical issues in 1H NMR spectroscopy: N-acetyl-L-aspartate, creatine, and choline. NMR